

Abstract

BCLxl, a member of the B-cell lymphoma-2 (BCL-2) family, is a protein that plays a key role in cell survival by preventing mitochondrial outer membrane permeabilization (MOMP). The ability of BCLxl to block apoptotic signals in the cell has been positively linked to tumorigenesis. Earlier *in vivo* experiments in the lab using mouse models showed the significance of individual domains within BCLxl's protein structure for dictating oncogenic potency. The Bcl-2 homology (BH)-4 domain of BCLxl has been shown to be essential in the anti-apoptotic functionality of BCLxl and certain residues within the BH4 domain of Bcl-2 are significant to the pro-survival potency of the protein. Site-directed mutagenesis was used to induce point mutations of conserved residues within the BH4 domain of BCLxl. Successful mutations would be used in ongoing *in vitro* experiments to further analyze the biochemical functions of BCLxl.

Introduction

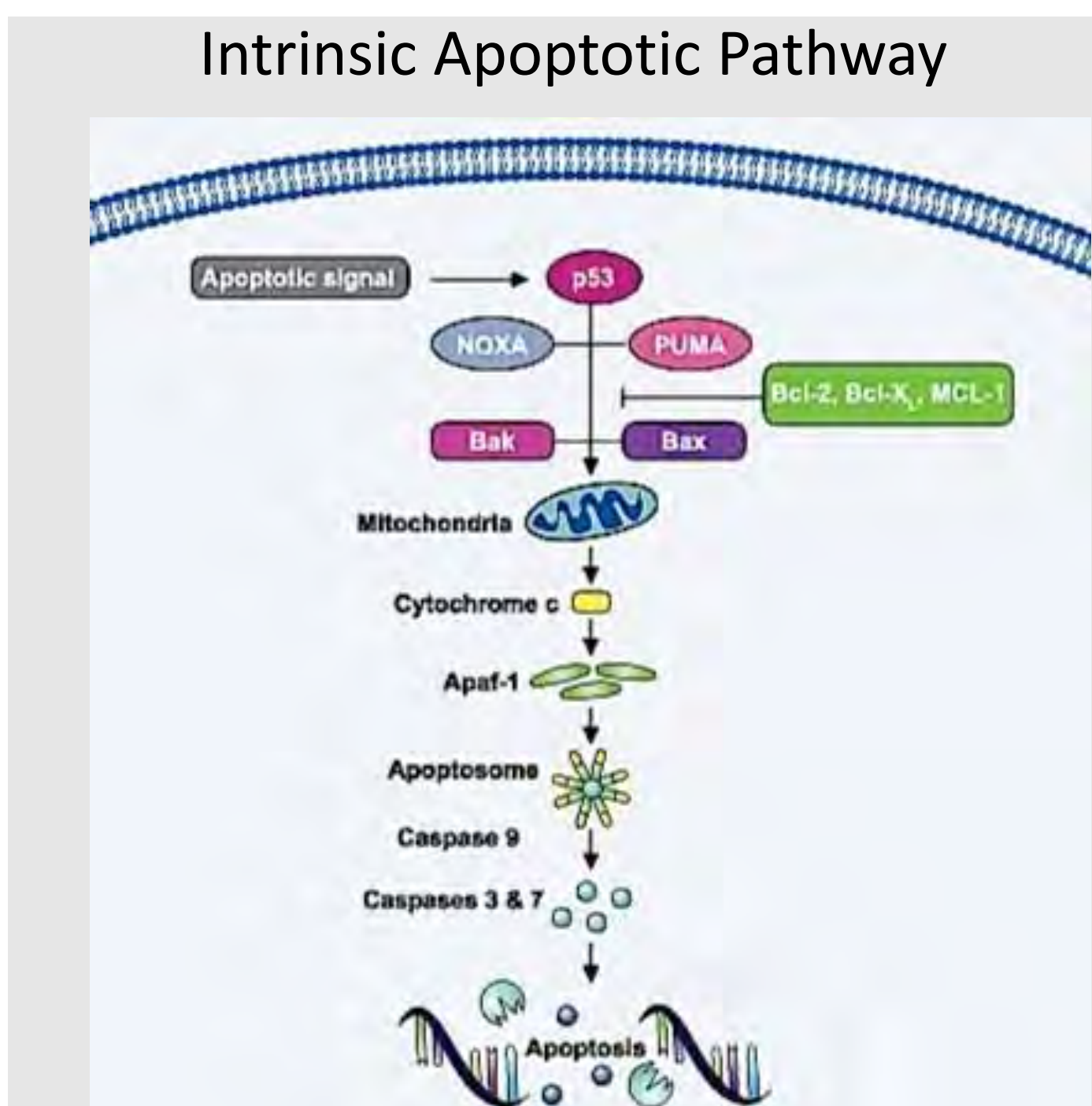


Figure 1. Intrinsic apoptotic pathway: directed by Bcl-2 protein mediation of mitochondrial outer membrane permeabilization.

The B-cell lymphoma 2, or BCL2, family of proteins plays a large role in the determination of cell death and cell survival. The family of proteins is divided into pro-apoptotic proteins, such as BAX and BAK, and anti-apoptotic proteins, such as BCL2 and BCLxl. Pro-apoptotic proteins promote cell death via mitochondrial outer membrane permeabilization (MOMP) whereas anti-apoptotic proteins inhibit MOMP and can drive tumorigenesis. Thus the ability to regulate cell death is a critical area of research in developing novel therapeutics for cancer. Anti-apoptotic members of the BCL2 family have four conserved BCL2 homology domains: BH1, BH2, BH3, and BH4. The structural variations between the members of the BCL2 family is likely responsible for the difference in functional activity of these proteins. The first three homology domains are highly conserved, whereas the BH4 is much less well conserved, suggesting that the BH4 domain is significant in determining the potency of the individual BCL2-like gene. Chimeric genes were developed to further determine the role of BH4 in dictating *in vivo* oncogenic potency of BCLxl.

Survival Curves of *In vivo* BCLxl/BCLb Chimeric Constructs

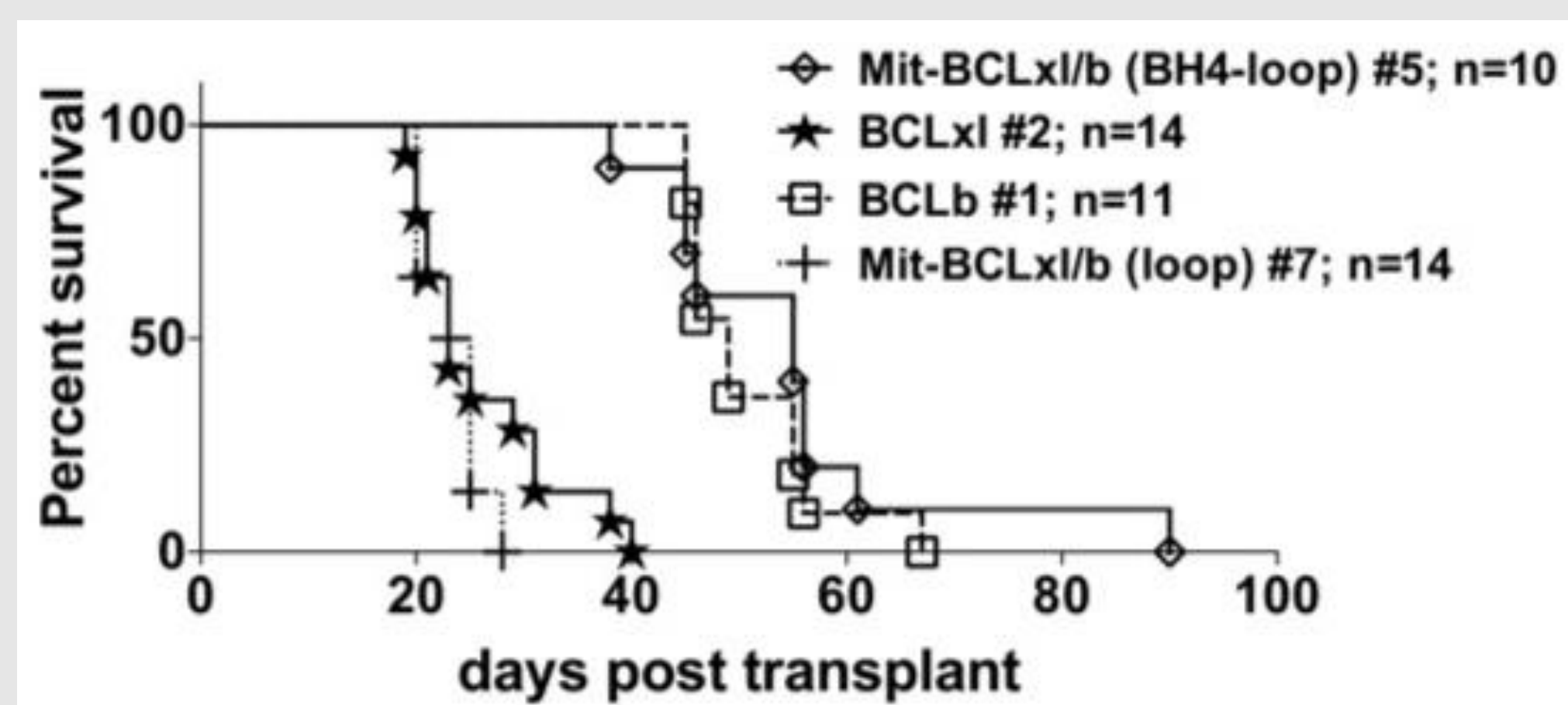


Figure 2. *in vivo* BCLxl/BCLb chimeric construct survival curves showing percent survival post transplant for mice infected with BCLb to be similar to those infected with construct #5, and separately, percent survival for those infected with BCLxl similar to those infected with construct #7.

Methods

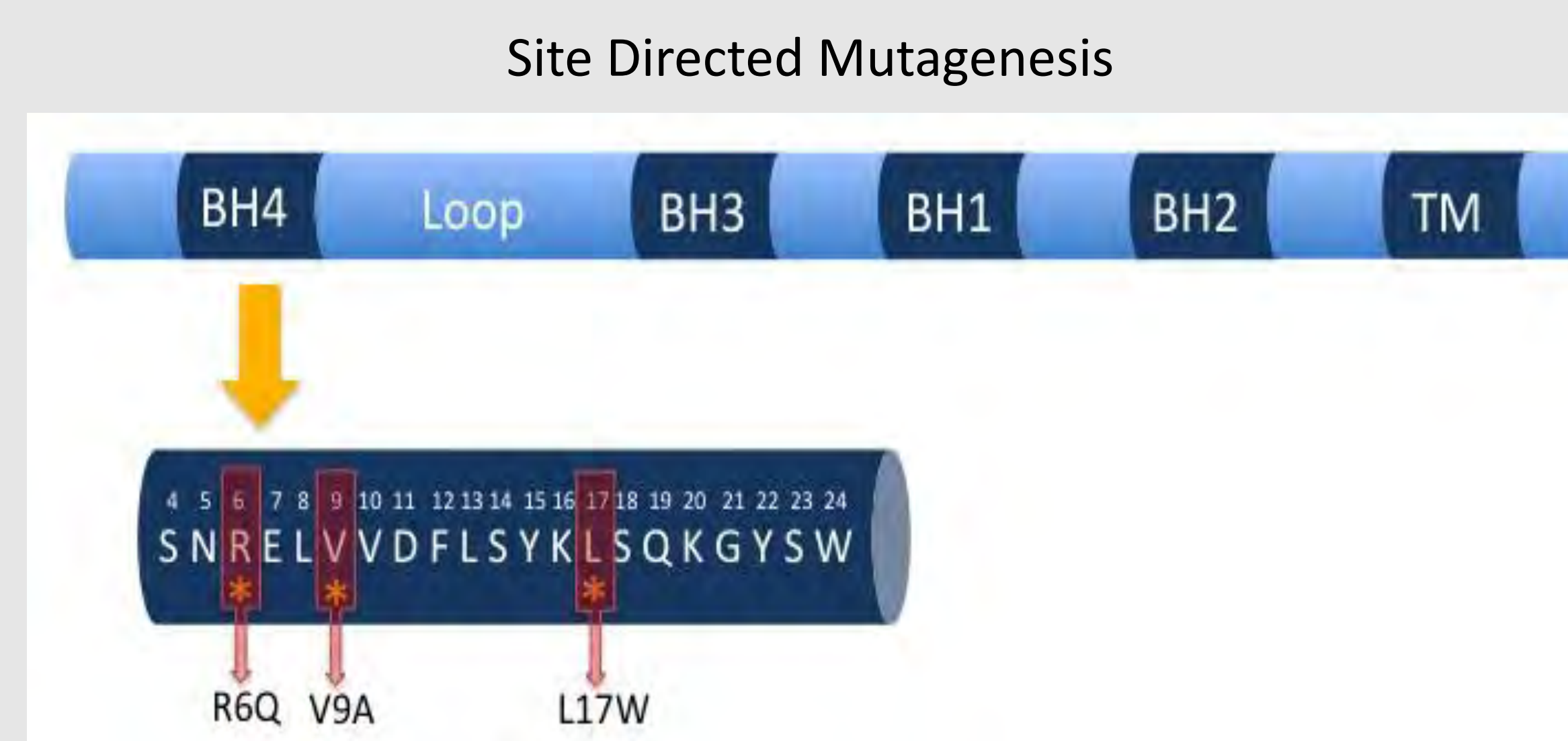


Figure 3. Point mutations of conserved residues in the BH4 domain of BCLxl are proposed to significantly impair the anti-apoptotic functionality of BCLxl. These mutations include replacements at the 6th, 9th, and 17th residues with glutamine, alanine, and tryptophan, respectively.

BCLxl and BCLb Chimeric Constructs



Figure 4. Structures of BCLxl (construct 2) and BCLb (construct 1) and chimeric constructs. Construct 5 includes the BH4 and loop domains of BCLb; construct 7 only includes the loop domain of BCLb.

Previous studies have also shown that substitutions of residues in the BH4 domain of BCL2 significantly impaired function, reducing the cell survival activity. Homologous residues were identified in the BH4 domain of BCLxl in order to perform a similar experiment to test cell survival with a mutant BCLxl gene. Site directed mutagenesis was performed using oligonucleotides containing the specific altered residues.

Western Blot of MIT and MIT Constructs



Figure 5. The western blot for FLAG and western blot for FLAG with immunoprecipitation of FLAG tagged proteins examining the relative expression of MIT constructs versus MIG constructs.

IP and Western Blot of MIT and MIT Constructs



In vivo experiments have found that MIT constructs express in lower levels than MIG constructs. Using *in vitro* experiments, where MIT and MIG vectors containing constructs 1, 2, 5, and 7 were transfected into 293T cells, we were hoping to show low expression was due to inherently low expressions or instability of the gene insert.

Conclusions and Future Directions

Point mutations via site directed mutagenesis will be utilized in future experiments to further examine the potency of mutated BCLxl. Once mutated BCLxl DNA is successfully generated, cell viability assays may be used to test cell survival.

Further studies will also be done to resolve the low expression of MIT BCLxl/BCLb constructs.

Acknowledgements

Research is supported by grant R25-CA-134283 from the National Cancer Institute. Many thanks to Dr. Levi Beverly and members of the Beverly lab for their mentorship and guidance.



Recombinant Expression of Codon-Optimized ANAPC2 and ANAPC11

James A. Stewart, Mark Doll, and J. Christopher States

Pharmacology and Toxicology, University of Louisville School of Medicine

Abstract

The current mitosis disrupting chemotherapeutics on the market today are spindle poisons that attack mitotic spindle formation and activate the spindle assembly checkpoint (SAC). Activation of the SAC causes inhibition of the Anaphase Promoting Complex/Cyclosome (APC/C), an E3 ubiquitin ligase. Prolonged mitotic arrest leads to cell death. Direct inhibition of the APC/C will lead to mitotic arrest and could eliminate the need for a functional SAC. APC/C inhibition by the disrupting interaction between its subunits ANAPC2 and ANAPC11 will lead to its loss of function and cause cell apoptosis. Using homology structures for *in silico* screening identified several compounds that could disrupt the ANAPC2/ANAPC11 binding. Thermoflour assays can be used in order to show the on target binding of these compounds and give an order of binding affinities. Previous attempts at expression and purification of recombinant ANAPC2 and ANAPC11 using human cDNA sequences failed. Therefore, codon usage in the ANAPC2 and ANAPC11 cassettes was optimized for *E. coli*. Codon optimized recombinant ANAPC2 and ANAPC11 cassettes were cloned into the IMPACT expression system as N-Terminal constructs in pTYB21. IPTG concentration and growth temperature and time were tested in order to find optimal expression conditions. Production of purified recombinant ANAPC2 will allow binding assays to be run to test compound binding affinities. Compound binding to ANAPC2 with high affinity may displace ANAPC11 from ANAPC2/ANAPC11 complexes. Evidence of displacement will demonstrate the APC/C as a new target for future chemotherapeutic drugs. Partially supported by NCI grant R25 CA134283 to the University of Louisville.

Introduction

Cancer remains the second leading cause of death in the United States with 585,720 new deaths estimated in 2014. Cancer is the unregulated growth of cells. While early detection and treatment continue to increase likelihood of survival, there remains a great need for better drugs.

Current mitosis disrupting chemotherapeutics such as paclitaxel target mitotic spindle and rely upon a functional spindle assembly checkpoint (SAC) to induce mitotic arrest. Activation of the SAC inhibits the anaphase promoting complex/cyclosome (APC/C), the master regulator of mitosis. SAC mutations enable resistance in cancer cells to current drugs targeting mitotic spindle.

Direct inhibition of the APC/C can alleviate the need for a functional SAC. APC/C catalyzes the ubiquitylation of cyclin B1 and securin thus deactivating CDK1 and allowing separation of chromatids enabling mitotic exit. Direct disruption of a functional APC/C will result in extended mitotic arrest thus sending the cell into apoptosis.

Previous studies identified compounds likely to bind ANAPC2 and disrupt formation of ANAPC2/ANAPC11 complex and thus disrupt APC/C function and induce mitotic arrest. A key step in developing these lead compounds into useful chemotherapeutics is demonstration of on-target binding by the compounds. These assays which require recombinant protein.

Previous attempts at expressing recombinant ANAPC2 and ANAPC11 using human cDNA sequences in *E. coli* were unsuccessful. Codon usage was optimized for *E. coli* in an effort to improve expression.

Hypothesis

Optimization of codon usage in human ANAPC2 and ANAPC11 sequences will enable robust expression of recombinant proteins.

Methods

Figure 1. APC/C Role in Mitosis

In late prophase(A) the activator subunit Cdc20 is brought to the APC/C by a functional SAC. The enzyme separase is inhibited by securin. The inhibition allows cohesins to stay bound to the sister chromatids. In metaphase (B) the chromatids line up along the metaphase plate. The Cdc20 is released from SAC and binds to the APC/C targeting it to ubiquitylate securin, targeting it for degradation and thus activating separase. At this stage inhibition of the ANAPC11 binding to ANAPC2 could prevent activation of separase. In anaphase (C) the "glue" cohesins are cleaved by the active separase enzyme. The cleavage allows the sister chromatids to separate to opposite poles of the dividing cell. Figure courtesy of Douglas J. Saforo.

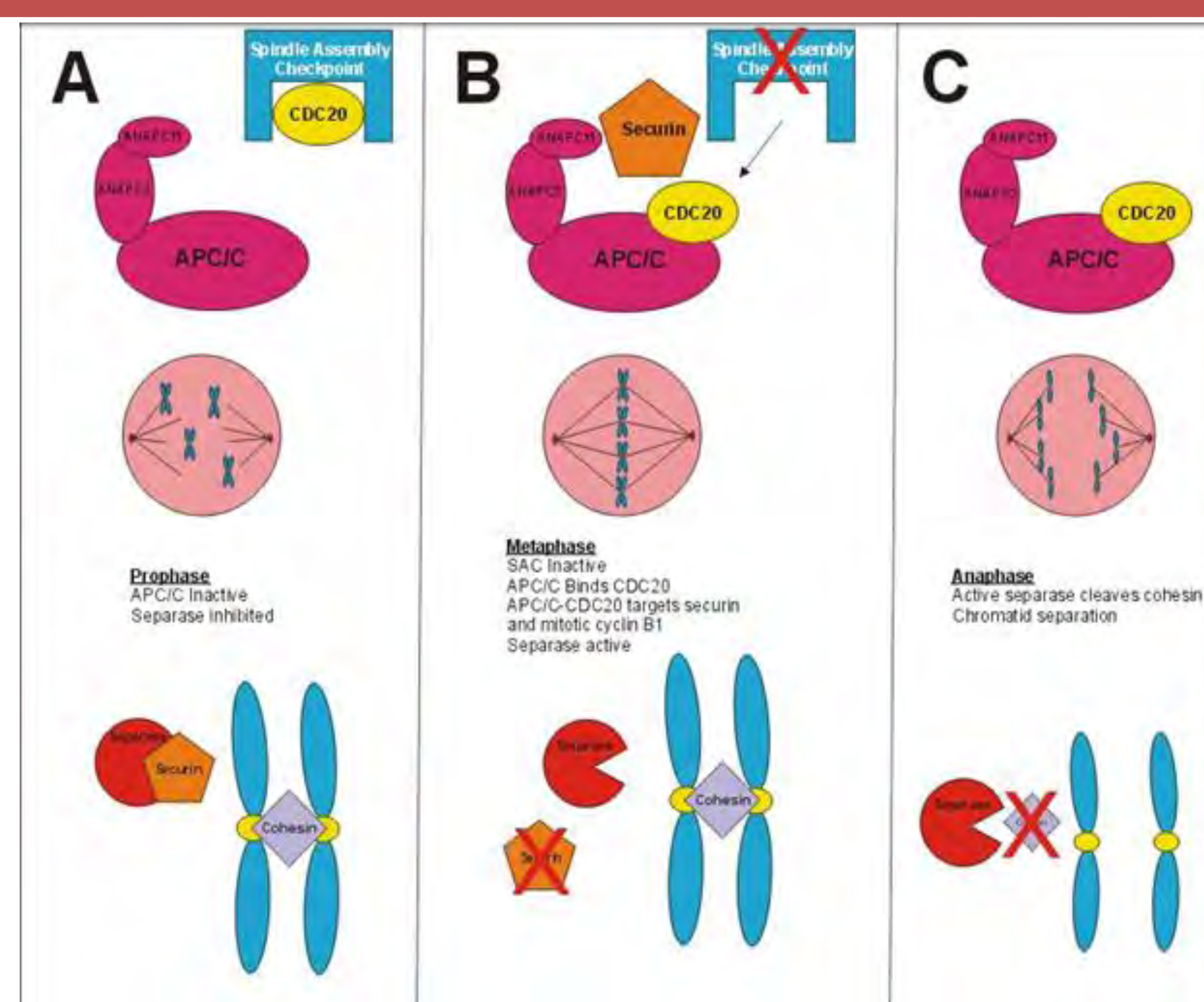


Figure 2. Cloning Genes Into The Vector

The pUC57 plasmids containing the optimized cassettes of ANAPC2 and ANAPC11 coding sequences were cut with restriction endonucleases to liberate the cassettes. ANAPC2: Used NdeI and BamHI. ANAPC11: used triple digest with NdeI, BamHI and EcoRI. The vector pTYB21 containing a self-cleaving intein tag was digested with NdeI and BamHI to remove the MCS. DNA fragments were separated by agarose gel electrophoresis and extracted from the gel. ANAPC2 and ANAPC11 fragments were ligated into the vector pTYB21 for expression. Once ligated into the vector, plasmid DNA from clones of both genes propagated in strain DH5 α were sequenced to confirm sequence fidelity and direction of ligation.

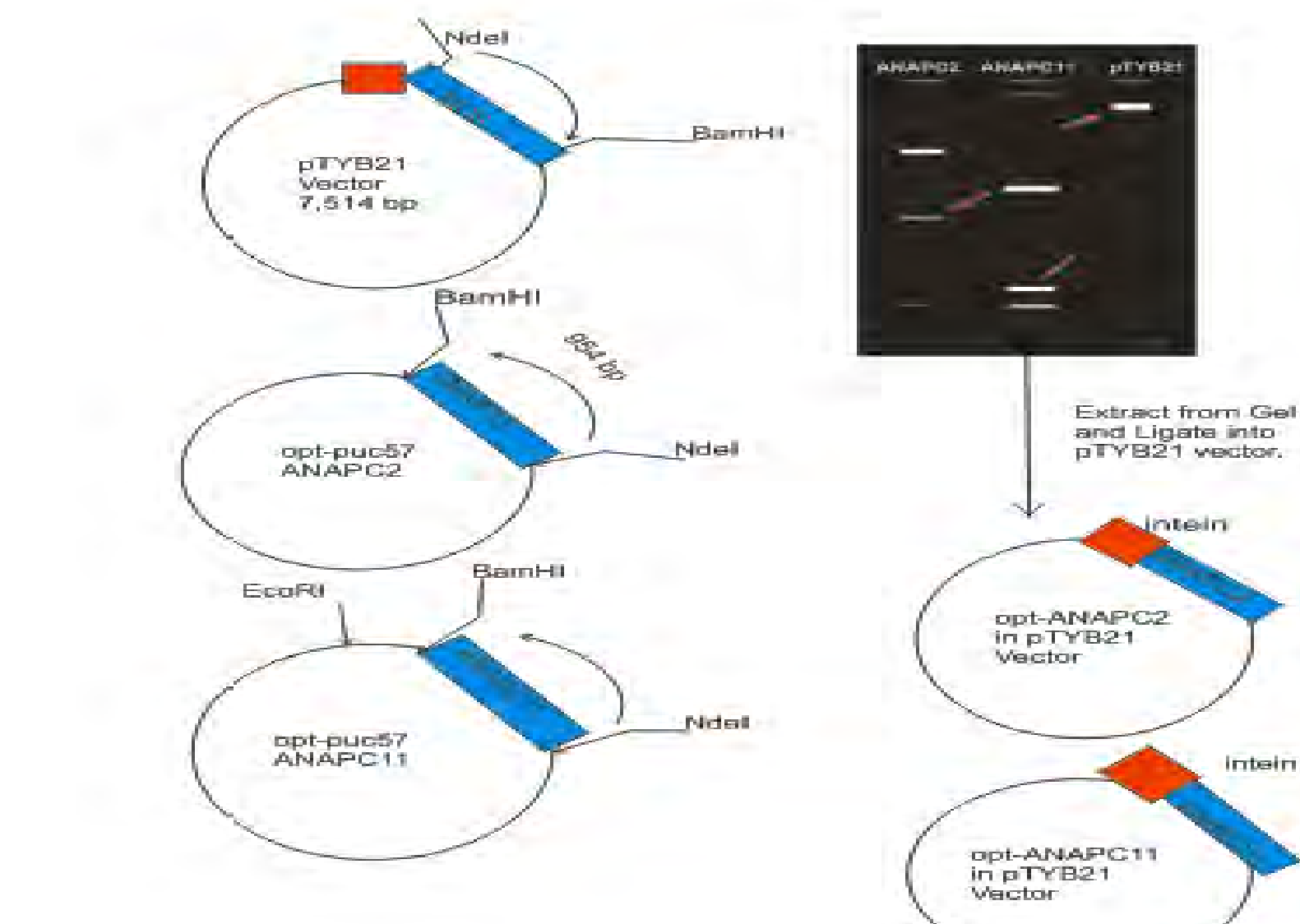
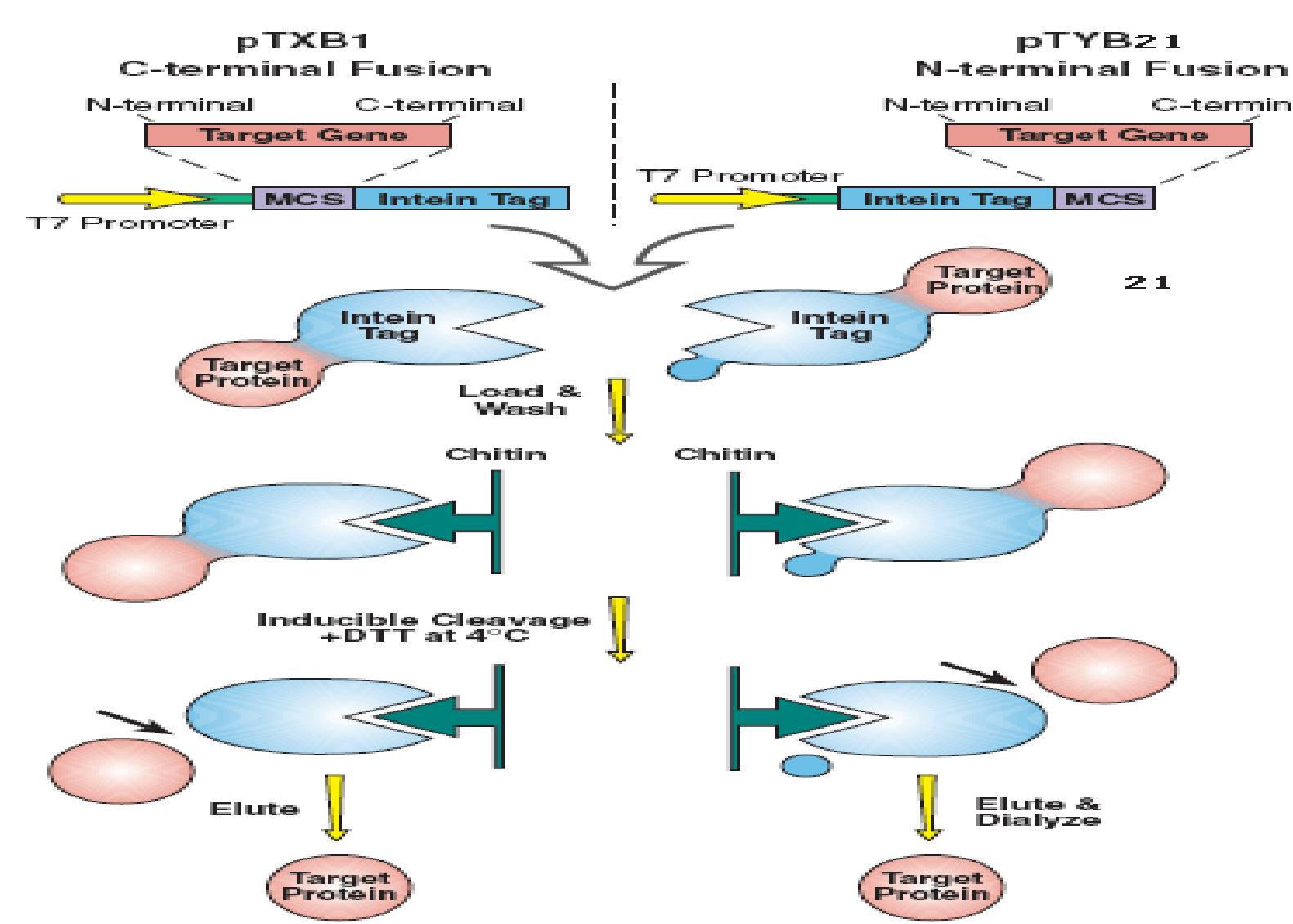


Figure 3. Protein Expression and Purification

The vectors containing both the ANAPC11 and ANAPC2 were transformed into new expression T7 cells. A variety of temperatures and IPTG concentrations were tested for maximum protein expression at different time points. A chitin binding domain attached to the self-cleaning intein will bind to a chitin column. Addition of DTT solution results in cleavage of the intein from the ANAPC2 and ANAPC11 proteins. At this point only the target protein will be in the flow through. Image obtained from NEB IMPACT™ manual.



Results

Figure 4. Restriction digest to isolate optimized ANAPC2 cassette and pTYB21 with NdeI and BamHI sticky ends to clone ANAPC2 cassettes. Left lane shows successful digestion of ANAPC2 plasmid with NdeI and BamHI. The middle band (red arrow) was extracted from the gel. Right lane is pTYB21 digested with NdeI and BamHI. The top band (red arrow) was extracted. Isolated fragments were ligated to form the expression plasmid.

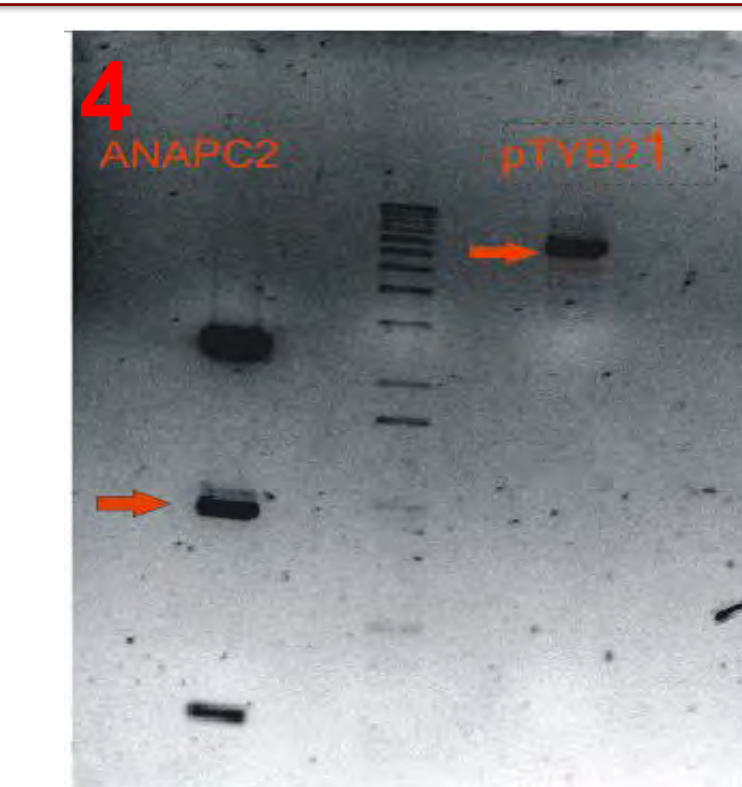


Figure 5. Restriction digest to isolate ANAPC11 cassette. A triple digest (NdeI, BamHI, EcoRI) of the optimized ANAPC11 plasmid was used to isolate the ANAPC11 cassette. The band at the blue arrow was extracted from the gel and ligated to pTYB21 vector isolated in Figure 4 to form the expression plasmid.



Figure 6. Time course for optimal protein expression. Samples of cell cultures were lysed directly in SDS sample buffer, resolved by SDS-PAGE and probed with anti-CBD antibody, and visualized using secondary antibody conjugated to horseradish peroxidase, incubate with ECL detection reagent, and image captured on x-ray film. Lane 1: 0 h induction (ANAPC2); Lane 2: 1 h induction (ANAPC2); Lane 3: 0 h induction (ANAPC11); Lane 4: 1 h induction (ANAPC11); Lane 5: 2 h induction (ANAPC11); Lane 6: blank; Lane 7: pTYB21 positive control for CBD. Sample in Lane 2 spilled into Lanes 1 and 3.

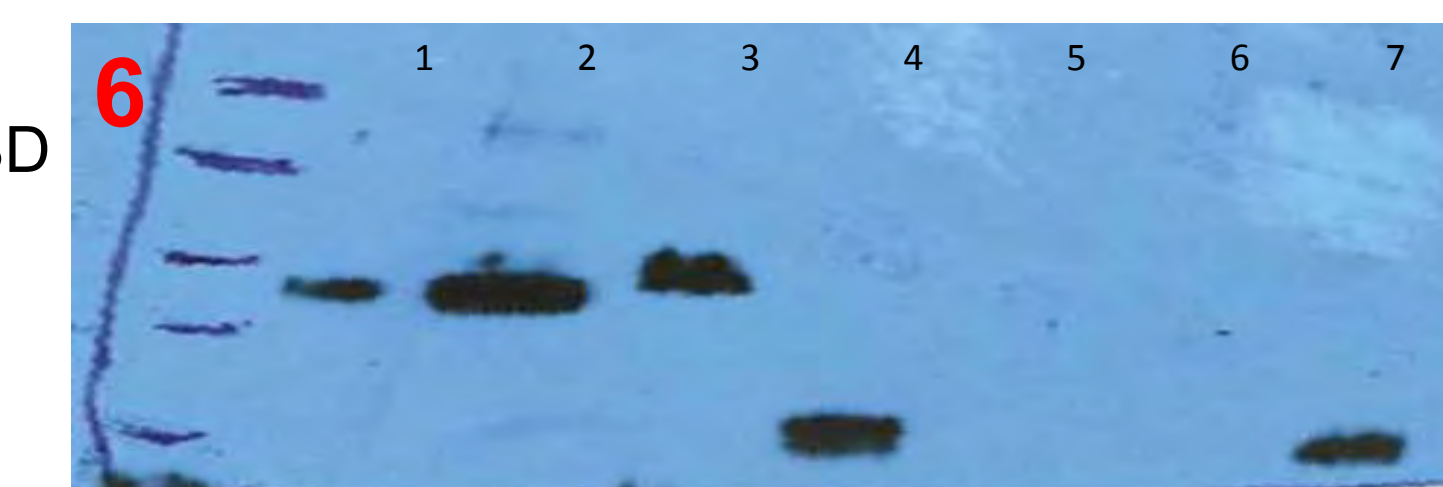
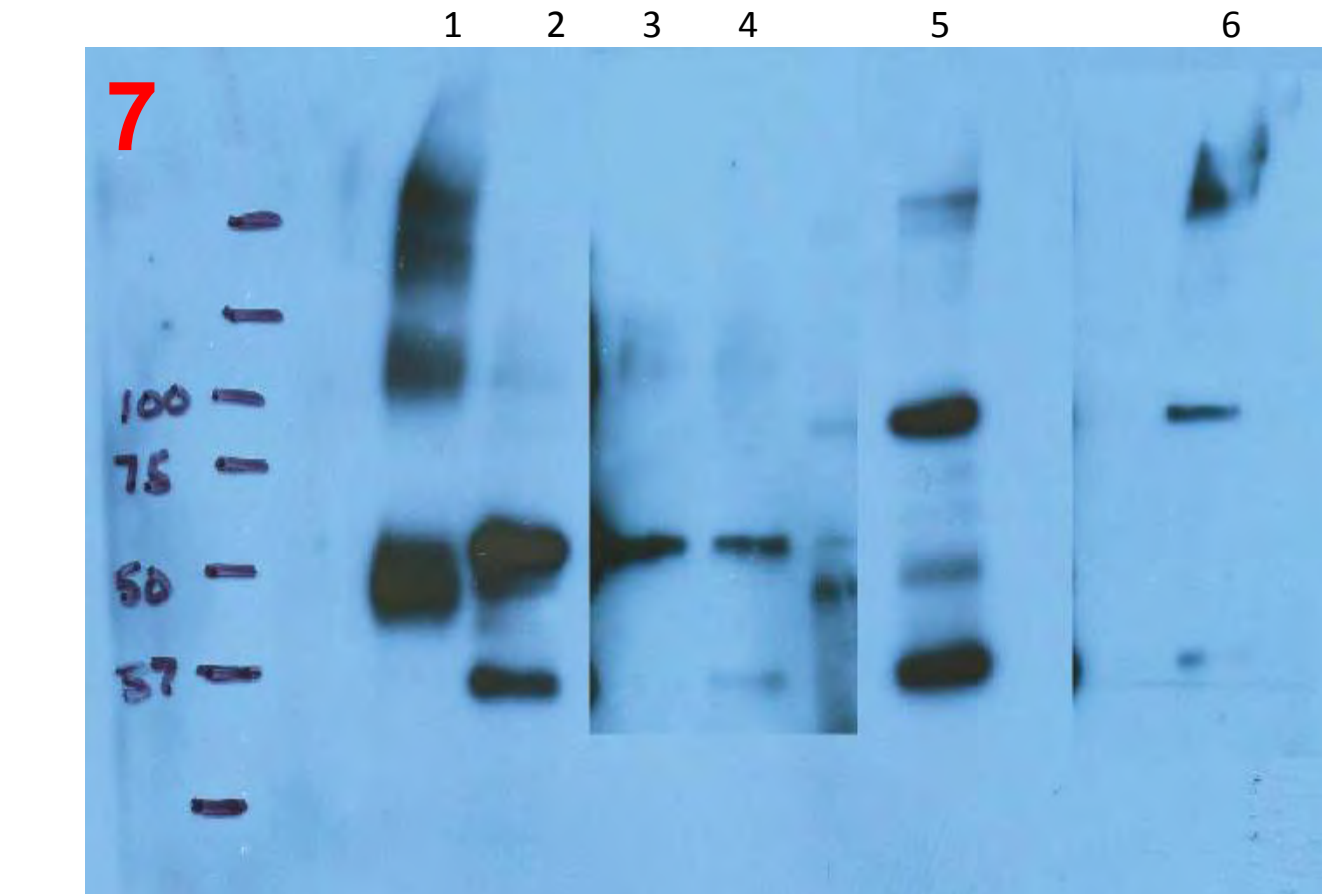


Figure 7. Sample analysis from protein purification. Cell cultures were grown and expression induced with IPTG. Cells were collected by centrifugation and resuspended for sonication and cell lysis. Cell debris was removed by centrifugation and the supernatant was run on a chitin column to isolate the fusion proteins. Columns were incubated with DTT to induce cleavage by the intein to liberate the ANAPC proteins. Lane 1: Beads from column after cleavage (ANAPC11 immediate induction); Lane 2: Beads from column after cleavage (ANAPC11, 37°C, 1 h); Lane 3: Lysate added to column for Lane 1; Lane 4: Lysate added to column for Lane 2; Lane 5: Beads from column after cleavage (ANAPC2, 37°C, 1h); Lane 6: Lysate added to column for Lane 5. Lanes 3, 4, and 6 are from the same gel but at a longer exposure time.



Conclusions

- Expression of ANAPC2 is most effective at 37°C with shorter expression times in order to make the protein soluble.
- Expression of ANAPC11 is most effective at 37°C with 1 hour of growth after addition of IPTG at any concentration.
- Purification has not been successful with a high enough yield to continue with assays yet.
- The proteins are soluble since they bound to the chitin beads. There is only cleavage in lane 1 of Figure 7. The proteins made it onto the column but have not cleaved in lanes 2 and 5.

Future Work

- Large scale purifications with the T7 express cells expressing the optimized ANAPC2 and ANAPC11 proteins.
- With the purified protein run thermoflour assays in order to test compound binding affinity to ANAPC2.
- Run thermoflour assays with ANAPC2/ANAPC11 complexes and test if compounds can displace ANAPC11.

Acknowledgement

- Partially supported by NCI grant R25 CA134283 to the University of Louisville.

Evaluation of coated gold nanoparticles targeted with Syndecan-1 for detection of pancreatic adenocarcinoma

Christopher Ullum, Anil Khanal, Shanice Hudson, Lacey R. McNally

Department of Medicine, University of Louisville, Louisville, KY

ABSTRACT

Purpose: Mortality of pancreatic cancer remains unchanged for the past four decades due in part to the inability to detect early stage tumors. Presently, there is no gold standard for early identification of pancreatic adenocarcinoma. Therefore, we sought to create a contrast agent which would identify pancreatic tumor cells using a newly emerging imaging system, Multi-spectral Optoacoustic Tomography (MSOT). Because this technology detects the thermoelastic expansion of highly absorbing particles, we developed two fully functional and stable gold nanorods to serve as this contrast agent.

Methods: Gold nanorods (GNRs) were synthesized via the seed-mediated method. To overcome the common detriment of gold nanoparticle aggregation, the GNRs were coated with mesoporous-silica (MS) or poly-acrylic acid (PAA). Coated GNRs were conjugated to Syndecan-1 peptide to facilitate detection of pancreatic cancer cells. Synthesized nanoparticles were characterized by Transmission Electron Microscopy (TEM), UV-Visible Spectroscopy (UV-vis), and Zeta-potential. The cellular uptake of nanoparticles was evaluated using Cytoviva Hyperspectral Imaging. Initial assessment of coated and targeted GNRs as potential contrast agents to detect pancreatic cancer was determined using tissue phantoms within the MSOT. Subsequently, mice bearing orthotopic pancreatic tumors were injected with syndecan-1 MS-GNR followed by MSOT imaging.

Results: The GNRs have an aspect ratio of 30:7 with MS-GNR and PAA-GNR containing a 10 nm mesoporous silica shell and 3 nm PAA shell, respectively. While the encapsulation of mesoporous-silica decreased the zeta-potential from +23 mV (CTAB-GNR) to -32 mV (MS-GNR), zeta-potential of PAA-GNR was -59.2 mV. Upon coating of mesoporous-silica and PAA, the UV-vis spectra showed a red-shift of 32 nm and 15 nm, respectively. Neither the MS-GNR nor PAA-GNR demonstrated aggregation for 2 days in comparison to the CTAB-GNR particles which aggregated within 1 h at pH 7.4. The Syndecan-1 MS-GNR particles were observed on the cellular membrane and facilitated detection of pancreatic cancer cells within the tissue phantom using MSOT. Syndecan-1 MS-GNR particles facilitated detection of orthotopic pancreatic via MSOT in mice.

Conclusion: Syndecan-1 targeted MS-GNR could serve as a potential contrast agent to facilitate detection of pancreatic tumors using Multispectral Optoacoustic imaging. Further studies will be conducted to conclude the location of GNR during cellular uptake.

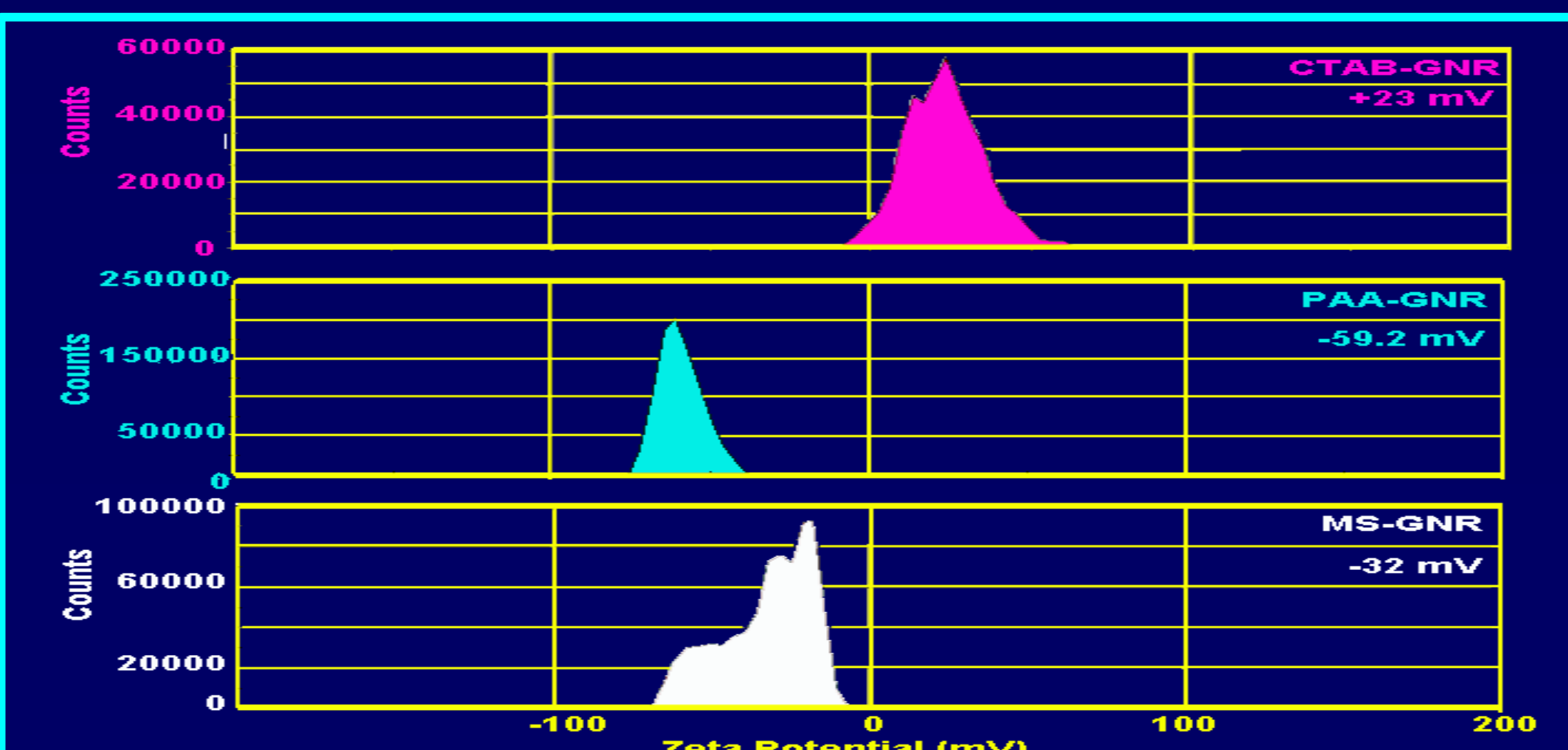
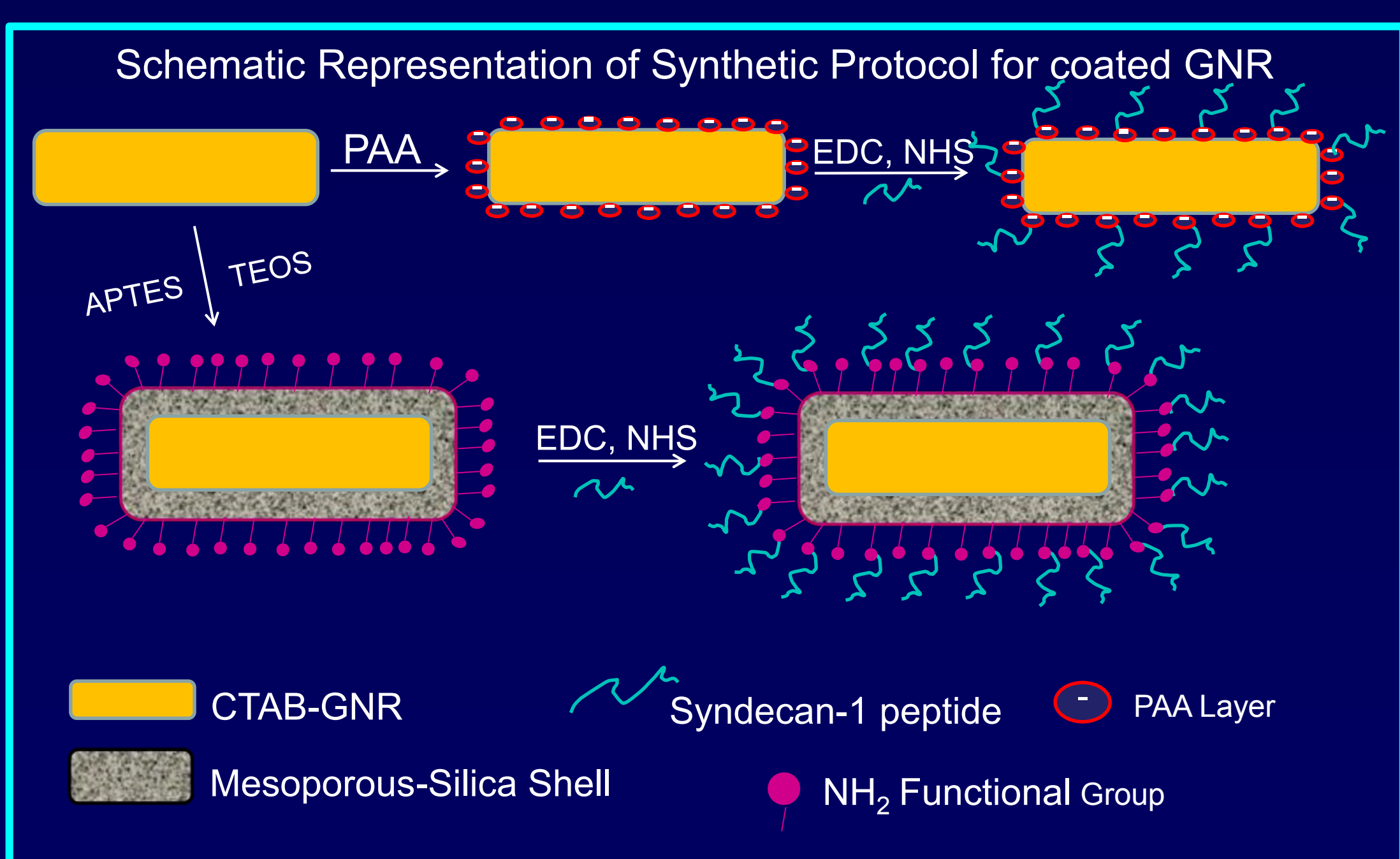


Figure 1: Zeta potential distribution of CTAB-GNR, PAA-GNR, MS-GNR.

RESULTS

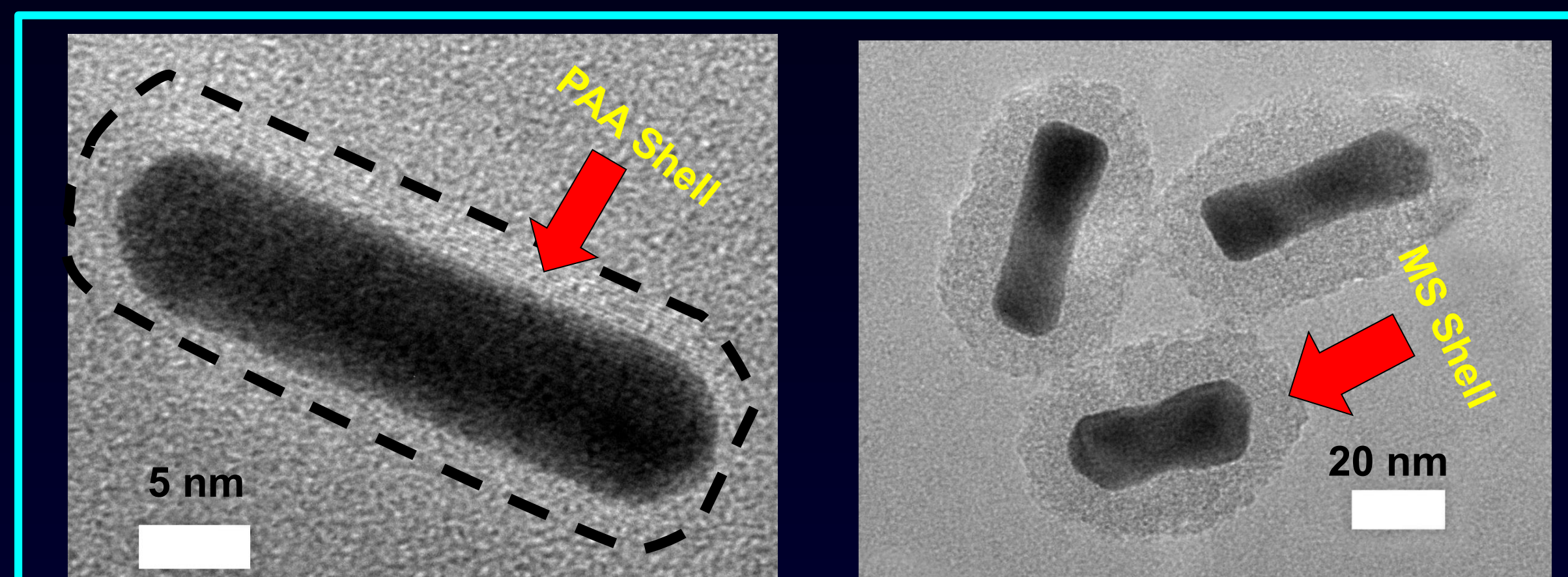


Figure 2: Transmission Electron Micrograph shows GNRs with poly-acrylic acid shell (PAA) and mesoporous-silica (MS) shell. (A) AuNRs were made with aspect ratio 30:7 and coated with a 3 nm poly-acrylic acid (indicated by - - line). (B) AuNRs were encapsulated with a 10 nm mesoporous-silica shell.

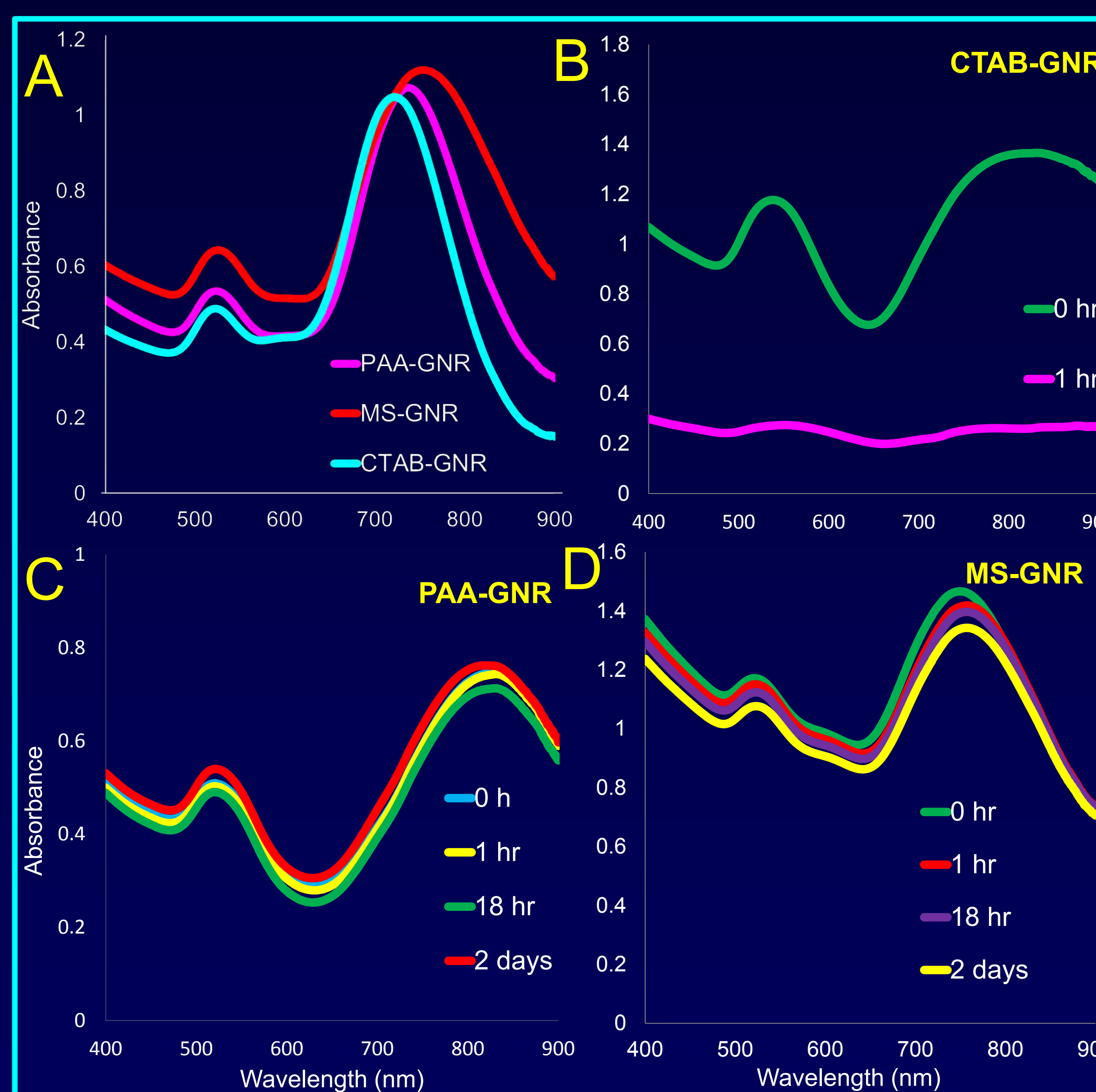


Figure 3: Absorption spectra of CTAB-GNR, PAA-GNR, and MS-GNR. (A) Poly-acrylic acid and mesoporous-silica coating was confirmed by a small red-shift of 15 nm and nm, respectively. (B) Instability and aggregation of CTAB-GNR is apparent after 1 hr. (C) Stability of PAA-GNR is shown up to 2 days. (D) Stability of MS-GNR is shown up to 2 days.

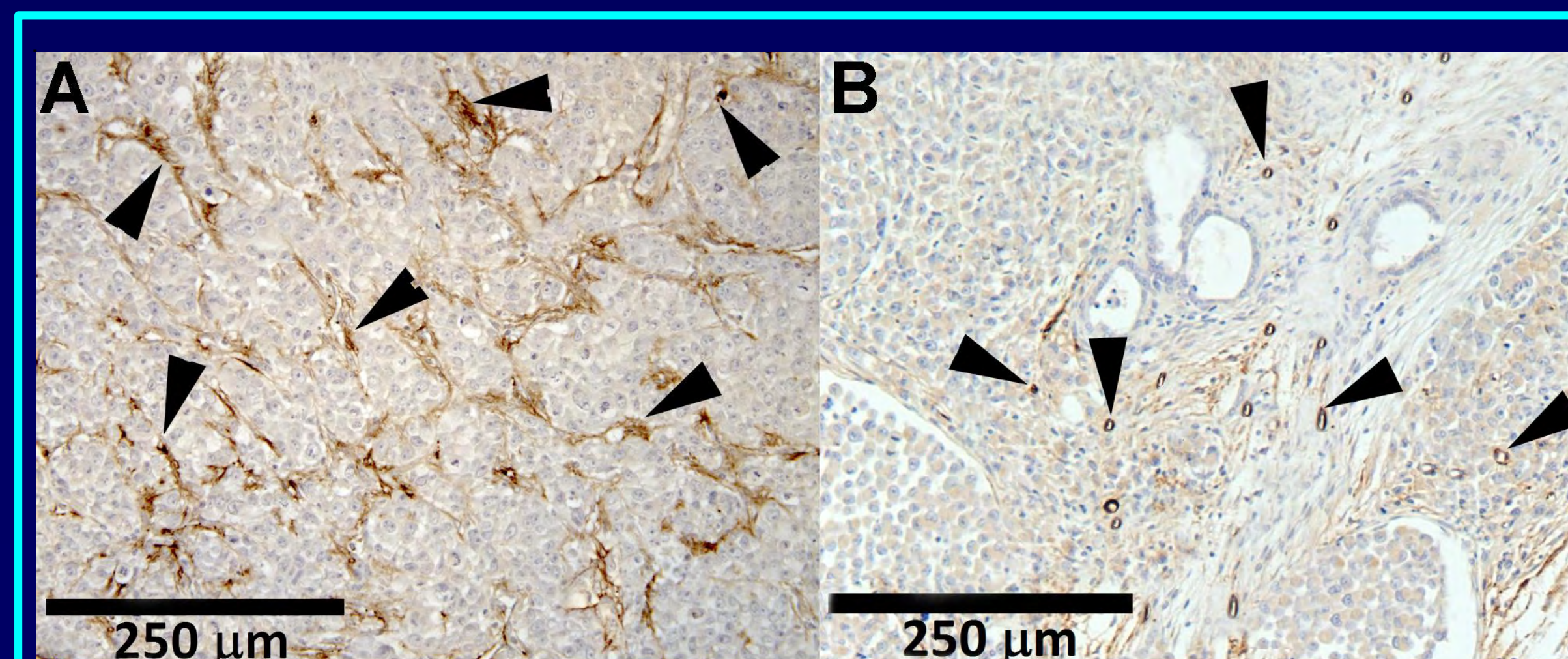


Figure 4: Vasculature of subcutaneous tumor vs. orthotopic tumor. (A) Brown coloring shows subcutaneous tumor stained with an endothelial marker, CD31 (indicated by arrow). (B) Shows orthotopic tumor with less vasculature. The explicit difference in vascular density indicates one of the pitfalls of subcutaneous tumors for the evaluation of nanotechnology.

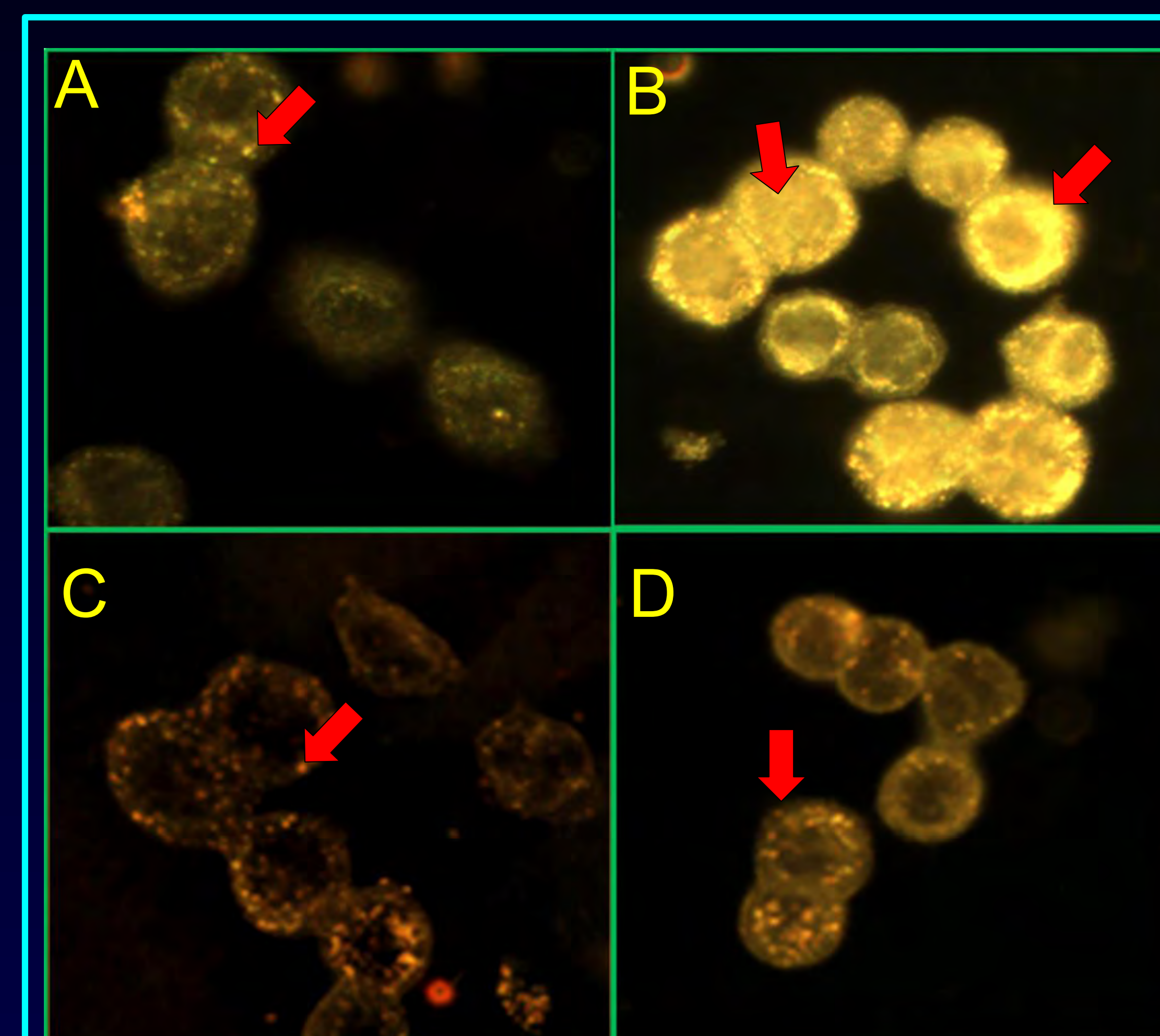


Figure 5: Cellular uptake of Syndecan-1 targeted MS-GNR was confirmed using Cytoviva Hyperspectral Imaging. S2VP10 cells were plated onto slides at a density of 1.0×10^5 cells per well. Cells were treated with particles ($6.5 \mu\text{g}/\mu\text{l}$) for 1h. Unattached particles were removed by washing with PBS and citrate buffers. Punctate foci indicate nanoparticle aggregation with possible endo- or phago-cytosis. Syndecan-1 targeted particles exhibited higher intensity with diffuse particle distribution throughout the cellular membrane. (A) No-ligand MS-GNR; (B) Syndecan-1 MS-GNR; (C) No ligand PAA-GNR; (D) Syndecan-1 PAA-GNR.

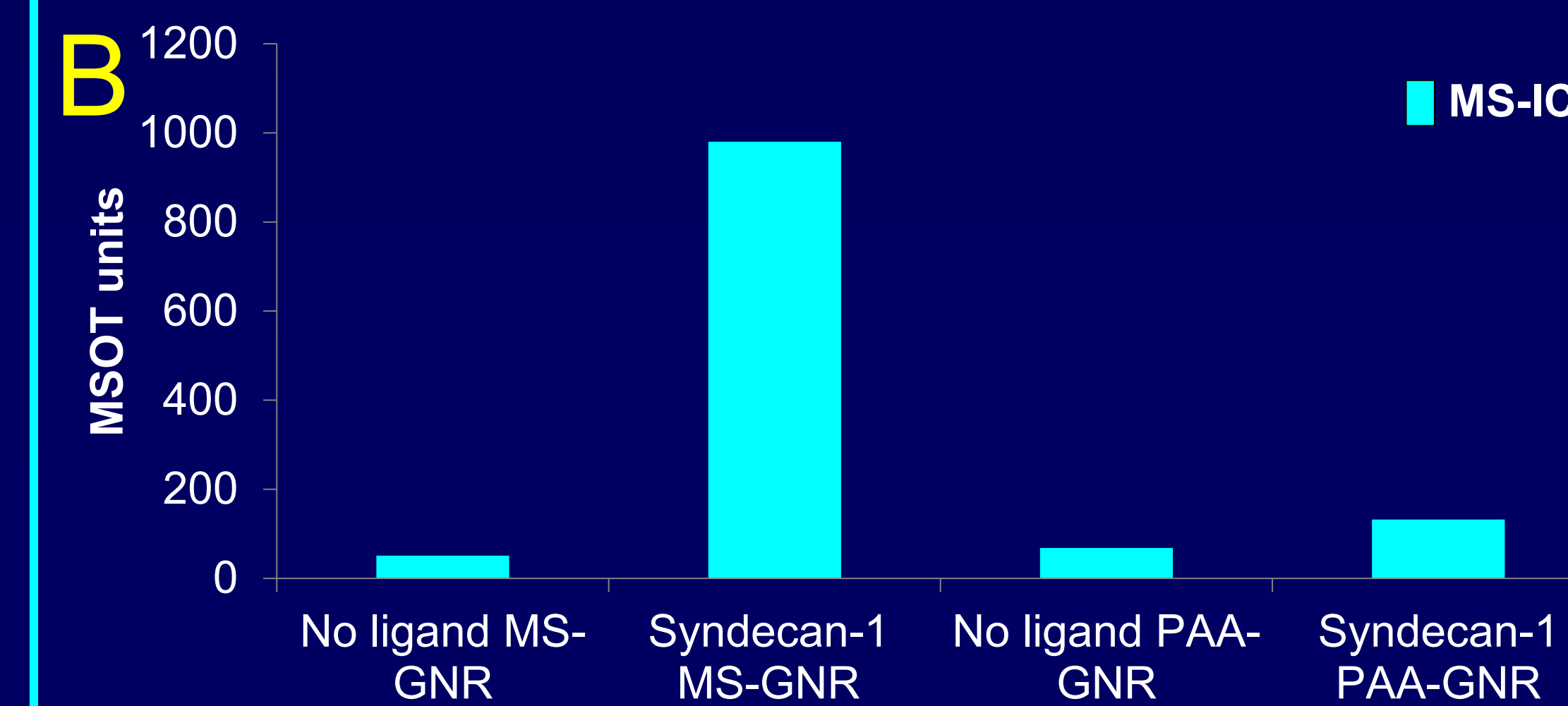
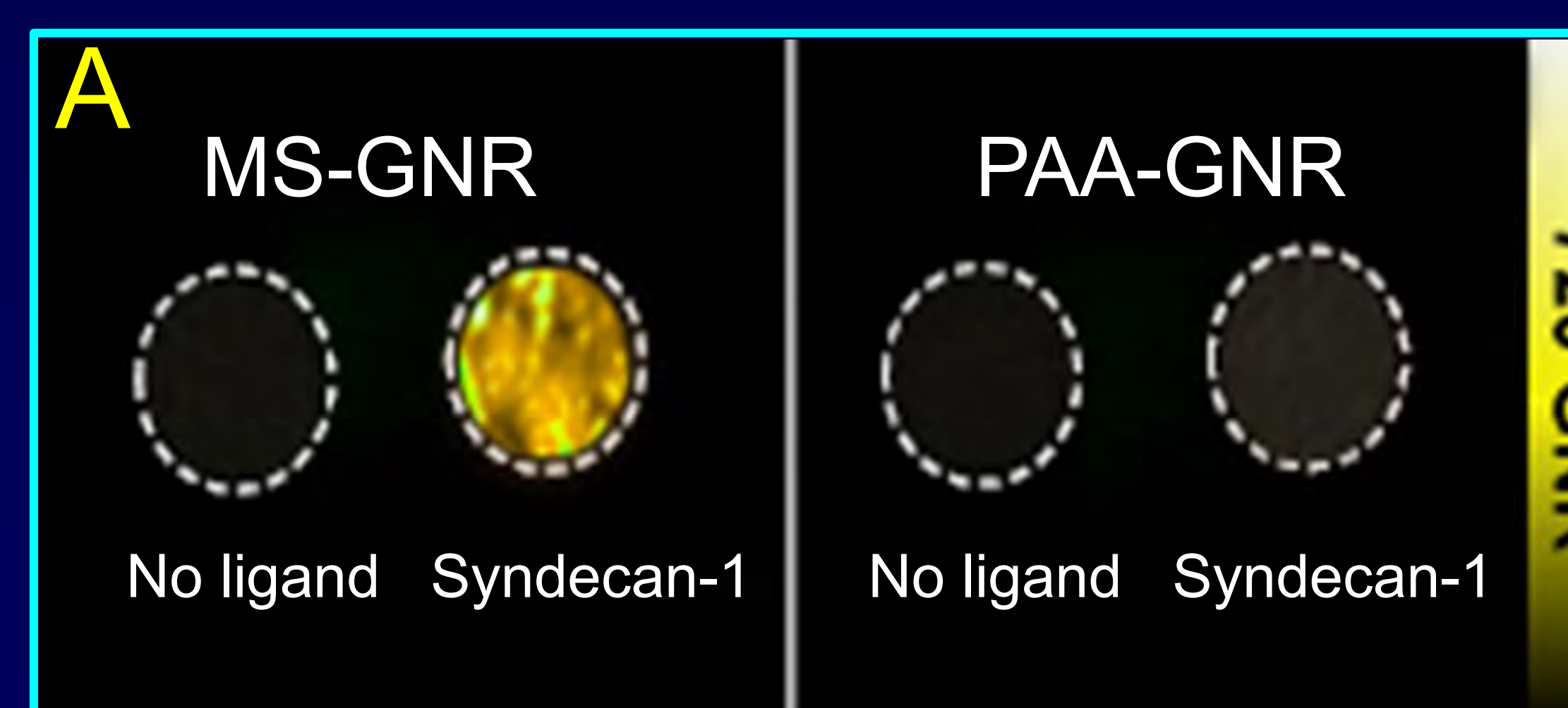


Figure 6: Visualization of ligand-targeted coated GNR in cells using phantoms with MSOT. Cells incubated with MS-GNR Phantoms are arranged with the negative control on the left and the positive control on the right. Cylindrical phantoms with a diameter of 2 cm were prepared using a gel made from distilled water, Agar, and an intralipid 20% emulsion (to simulate light diffusion in vivo). (A) Both ligand targeted and untargeted MS-GNR and PAA-GNR nanoparticles were incubated with S2VP10 cells and washed with PBS 3x. (B) Shows intensity of experimental phantoms in MSOT units (a.u.).

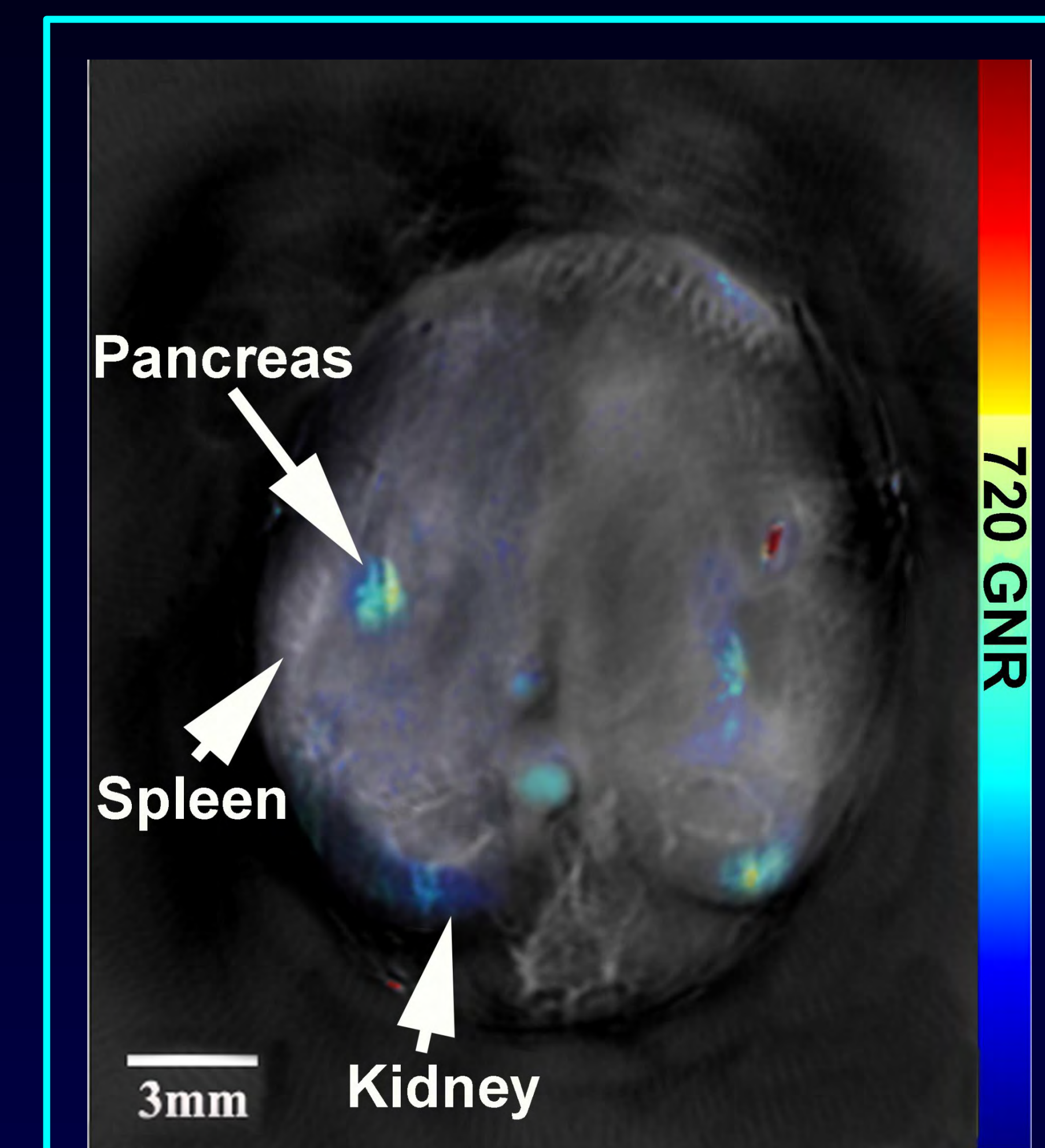


Figure 7: Identification of Syndecan-1 targeted MS-GNR in a pancreas tumor using Multispectral Optoacoustic Tomography. Nanoparticles ($1.1 \mu\text{g}/\mu\text{l}$) were i.v. injected into tumor bearing mice. At 4 hour post injection, mice were imaged based upon the 720 GNR UV-absorption spectra using MSOT. Images were reconstructed using backprojection and signal was determined using multispectral processing. A single slice is shown which contains pancreas, spleen, and kidney.

CONCLUSION

Conclusion: This study suggests that targeted gold nanoparticles detected using optoacoustic imaging could offer a more sensitive, specific, and non-invasive method for diagnosing and monitoring pancreatic cancer in both the preclinical and clinical setting. As the goal of the study was to overcome gold nanoparticle aggregation upon injection, both coatings were served this purpose. However, the MS coating proved to be superior to PAA to facilitate tumor cell binding as demonstrated by both the Cytoviva Hyperspectral Imaging and tissue phantoms. At present, the bright fringes on cytoviva images indicate aggregation of GNRs, while the defused and uniformity of light is receptor-mediated binding. Due to the limits of physical laws of optical microscopy, future research will need to be conducted to determine the location of conjugated GNR during cellular uptake.

FUTURE DIRECTIONS

To determine the exact cellular location of the GNR (cell membrane or intracellular), treated cells will undergo standard fixation and sectioned for Transmission Electron Microscopy. More *in vivo* studies will be conducted to determine to appropriate concentration of conjugated GNR and optimize imaging timing.

ACKNOWLEDGEMENTS

This work was supported by NIH/NCI R25-CA134283 and CA139050.

Abstract

Purpose: To better understand the epidermal growth factor receptor (EGFR) in the endocytic pathway and the effect of a small Sprouty2-derived peptide on the rate of degradation of EGFR, which impacts cell proliferation and wound healing.

Methods: Liposomes were synthesized and peptide (FITC-Ahx-IRNTNE{pTYR} TEGPTV) was encapsulated in the liposomes via freeze and thaw cycles. Liposomes were incubated with the S2VP10 human pancreatic cancer cell line. S2VP10 cells were also treated with digitonin to permeabilize the membrane and incubated with peptide at different concentrations. Efficiency of peptide uptake into the cell was determined by fluorescent microscopy. EGFR degradation levels upon EGF ligand stimulation at time points 0, 15, 60, and 120 minutes were measured through immunoblotting.

Results: Dynamic Light Scattering (DLS) and spectral evaluation of the liposomes confirm that synthesis of the liposomes and encapsulation of the peptide was successful. Fluorescent microscopy shows that liposomes offer an efficient delivery of the peptide into the cell. EGFR activity levels, quantified through immunoblotting, do not suggest an effect induced by the liposomes.

Conclusions: The methodology used for the synthesis and peptide encapsulation allows for successful encapsulation of the peptide. Liposomes are an effective method of delivering the peptide into the cell in a controlled, targeted manner.

Western Blot results do not reveal a significant effect of the peptide on EGFR activity levels in the cells. Future experimentation is required to determine the efficacy of the peptide.

Introduction

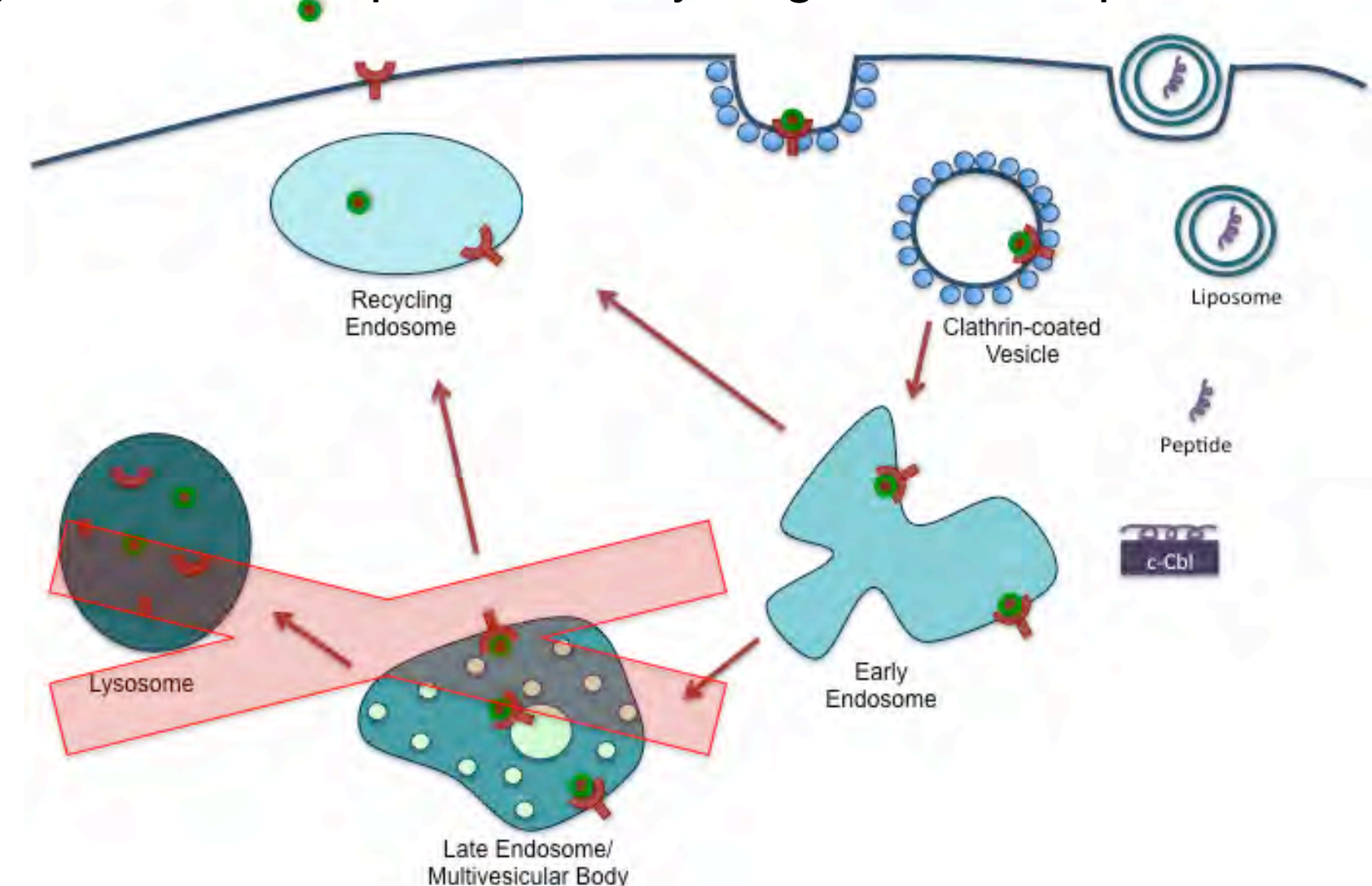
Cancer is the second leading cause of death in the US, accounting for one in every four. In 2014, 1,665,550 people are expected to be diagnosed with cancer, and 585,720 of these cases are expected to lead to death (www.cancer.org). Overexpression of the epidermal growth factor receptor (EGFR) is found in many carcinomas. Receptors may be endocytosed and follow the endocytic pathway from the early endosome to the lysosome for degradation, or they may be recycled back to the membrane by transport vesicles via transcytosis. C-Cbl binds to the phosphorylated receptor, which targets proteins for ubiquitination, leading to degradation of the receptor-ligand complex in the lysosome. Sprouty2 is a large protein that has been found to act as a c-Cbl inhibitor.

Hypothesis: Binding a small Sprouty2-derived peptide to c-Cbl will sequester it, preventing receptor ubiquitination, causing EGFR to be recycled to the plasma membrane and promote proliferation.

By learning how to manipulate basic cell mechanisms, we can better understand how to slow proliferation and make advances in cancer treatment.

Liposomes will be used to deliver the peptide into the cells by encapsulating the peptide in the core of the liposomes. Internalization of liposomes into the cell may occur through adsorption, lipid exchange, receptor-mediated endocytosis, or fusion (*Liposomes: A Practical Approach*). Liposomes will promote internalization of large molecules that would not otherwise be efficiently taken into the cell. Smaller liposomes, ideally 200 nm or smaller, have a longer circulation half-life and enhanced ability to internalize into the cells when compared with larger vesicles.

The objectives of this project are to: (1) synthesize liposomes with encapsulated Sprouty2-derived peptide; (2) internalize the liposomes in S2VP10 cells to release the peptide, which will in turn sequester c-Cbl; and (3) prevent EGFR from degrading in the lysosomes and promote recycling of the receptor back to the membrane.



Schematic 1. The hypothesis is that when liposomes deliver a Sprouty2-derived peptide intracellularly, sequestering c-Cbl, EGFR will recycle to the plasma membrane.

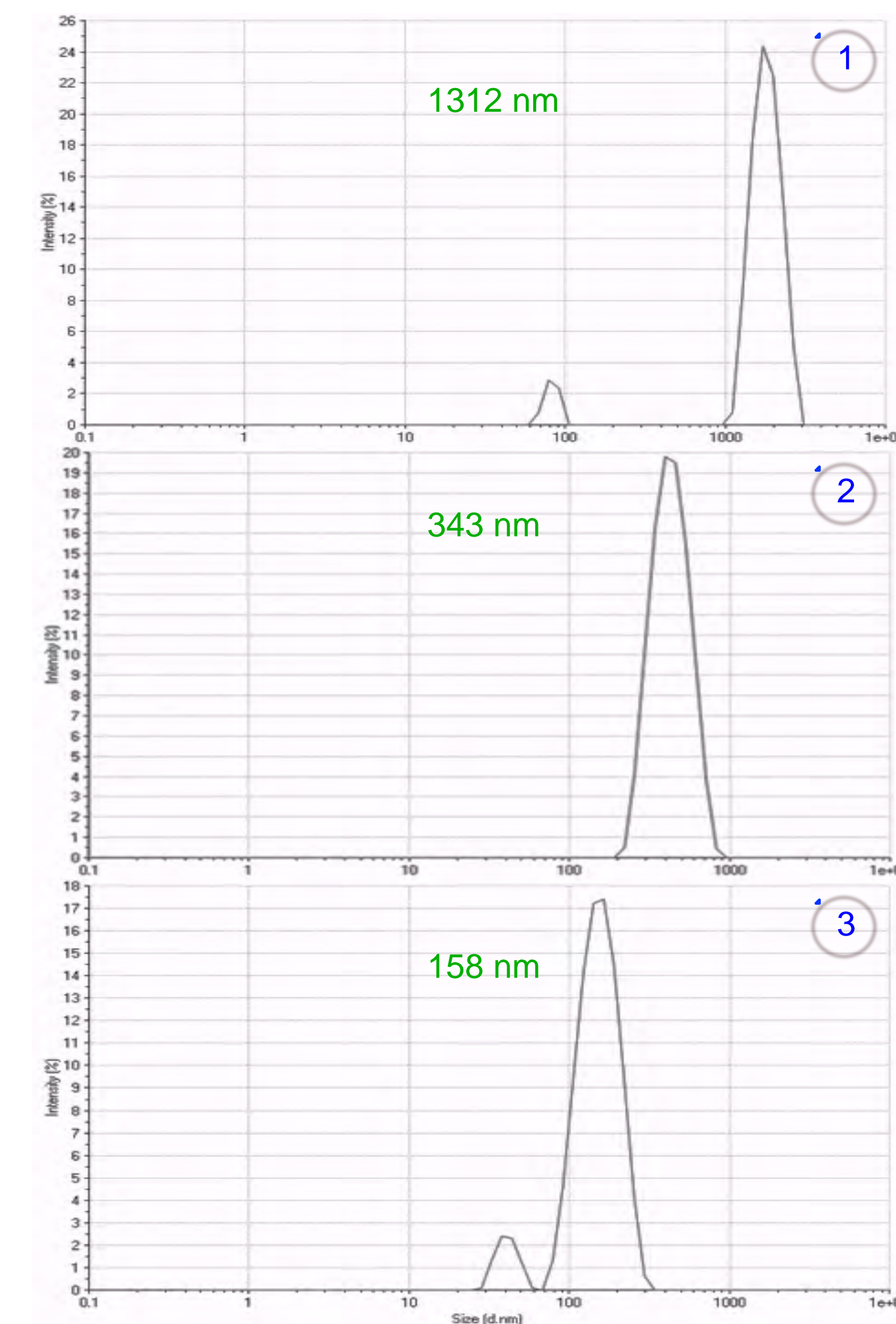
Flow Chart

Liposome Synthesis & Peptide Encapsulation



Figure 1

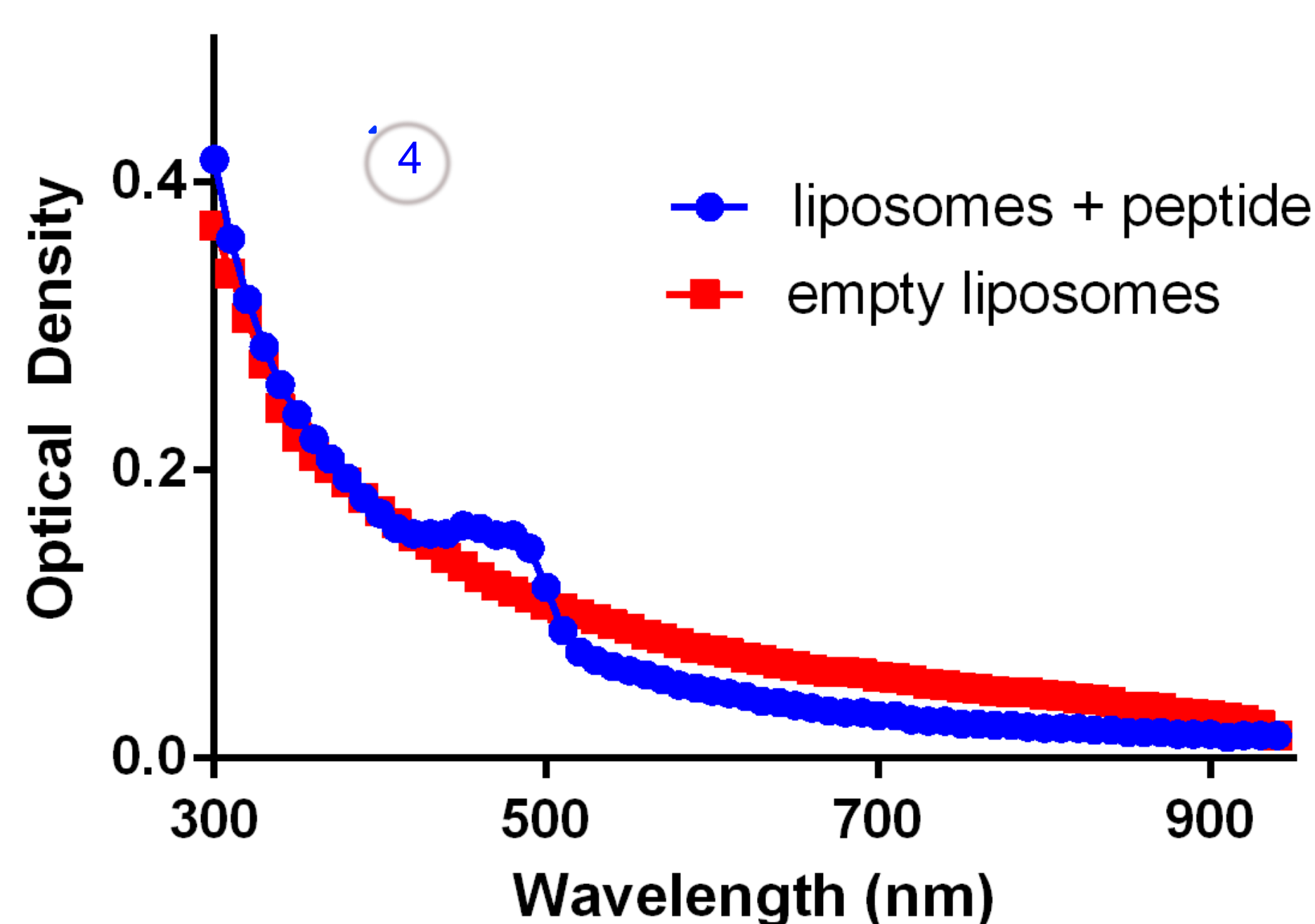
Liposome Size Distribution



Liposomes were synthesized using a 4:2:1 molar ratio of lipids PC:Cap:DOPE. The lipids were dissolved in chloroform, the solution was rotovapped then resuspended in a 0.9% NaCl solution. An aqueous peptide solution was added to the liposomes. 10 freeze and thaw cycles were completed to encapsulate the peptide. Extrusion and dialysis were performed. Size distributions of the liposome preparations were acquired using DLS following (1) synthesis, (2) peptide encapsulation, and (3) extrusion. Average size (Z-average) is given for each step.

Figure 2

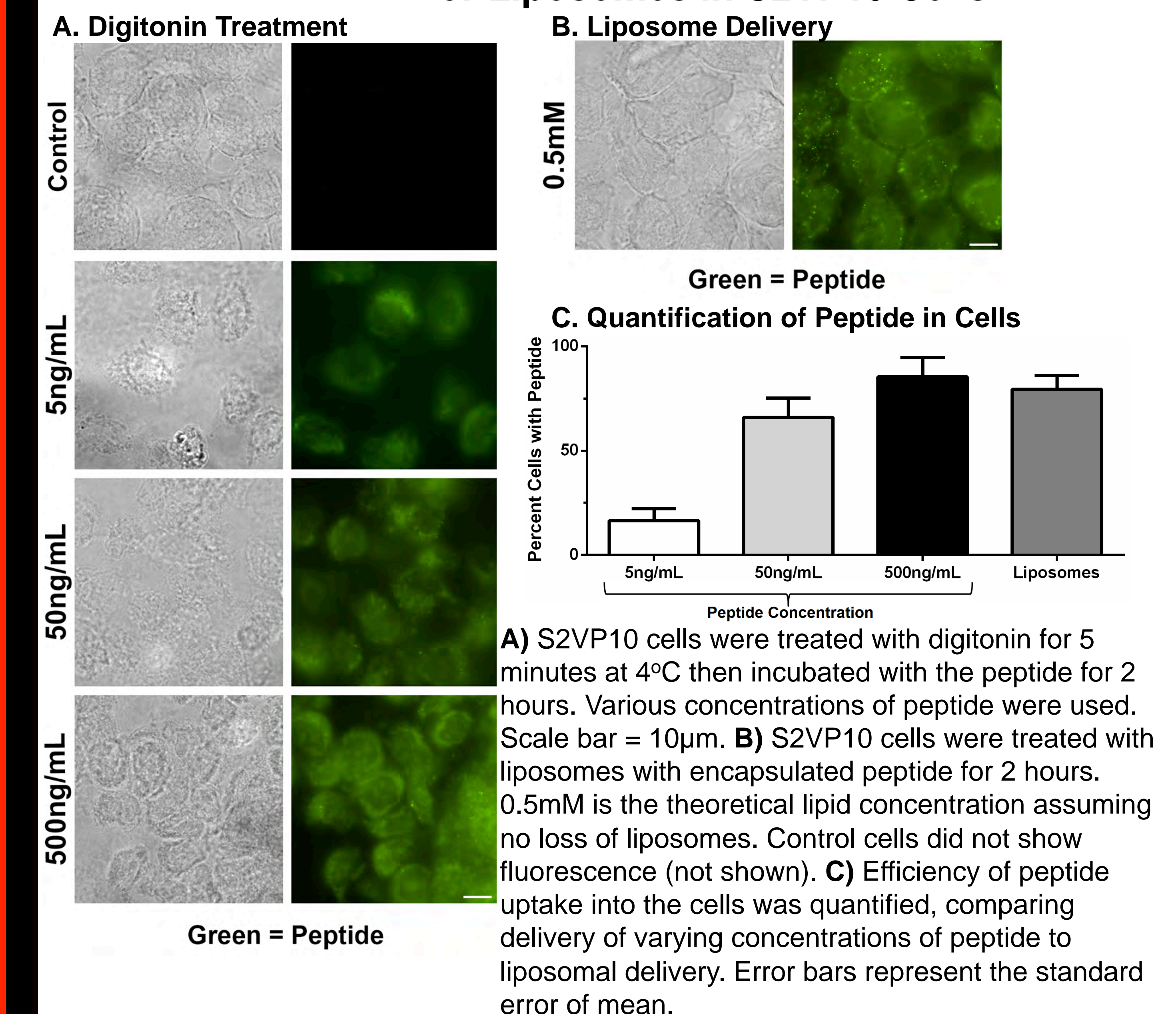
Spectral Evaluation of Liposomes



Dialysis uses a concentration gradient to remove the free peptide from the liposomes. Spectral evaluation of the liposomes was performed to verify the presence of peptide (4). The peak at 480 nm indicates peptide in solution, due to the FITC tag attached to the peptide. The presence of peptide upon dialysis confirms that the peptide was successfully encapsulated in the liposomes.

Figure 3

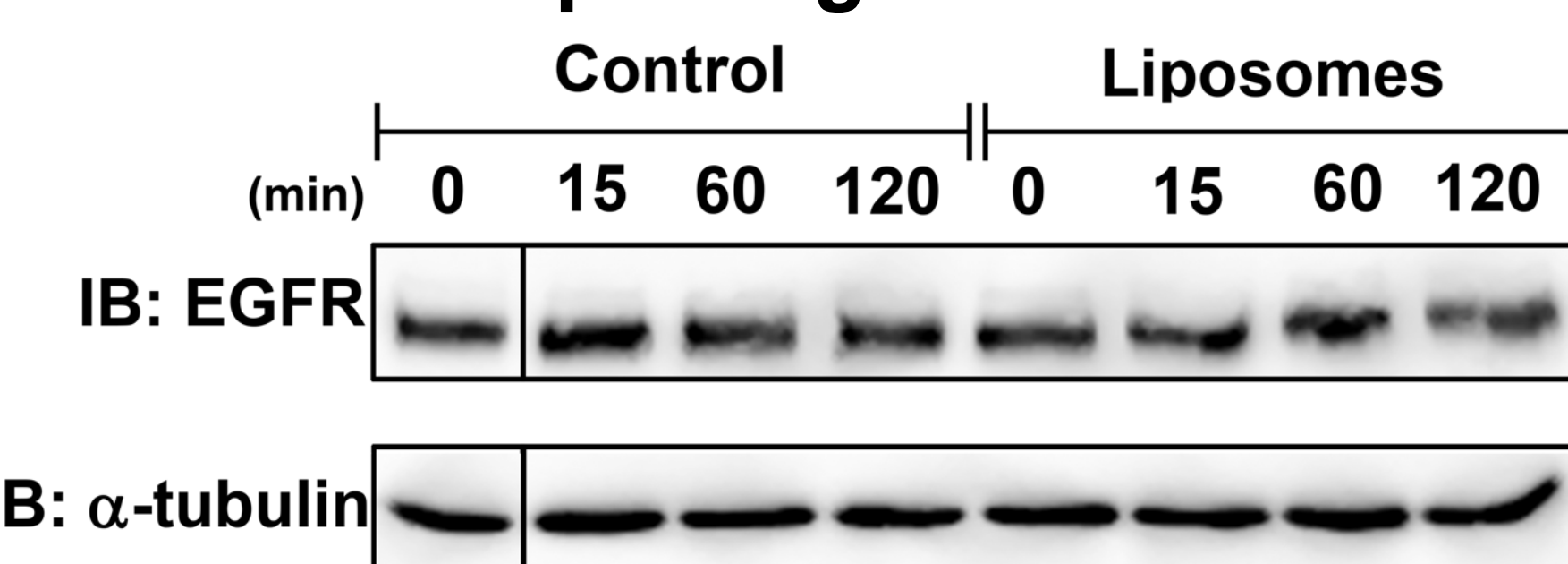
Peptide Delivery via Digitonin Treatment or Liposomes in S2VP10 Cells



A) S2VP10 cells were treated with digitonin for 5 minutes at 4°C then incubated with the peptide for 2 hours. Various concentrations of peptide were used. Scale bar = 10µm. **B)** S2VP10 cells were treated with liposomes with encapsulated peptide for 2 hours. 0.5mM is the theoretical lipid concentration assuming no loss of liposomes. Control cells did not show fluorescence (not shown). **C)** Efficiency of peptide uptake into the cells was quantified, comparing delivery of varying concentrations of peptide to liposomal delivery. Error bars represent the standard error of mean.

Figure 4

Evaluation of Receptor Activity Upon Ligand Stimulation



Upon treatment with liposomes, S2VP10 cells were incubated with EGF ligand at time points 0, 15, 60, and 120 minutes. Western Blot Assay was performed. The blot does not reveal a significant effect on sustaining EGFR activity in cells treated with liposomes.

Conclusions

- Freeze and thaw cycles facilitate encapsulation of the peptide in the liposomes, while also leading to the formation of smaller vesicles
- Extrusion is an effective method to control the size of the liposomes
- Liposome delivery is an effective method of delivering the peptide into the cells and is comparable to high peptide concentration delivery
- Liposome treatment did not result in sustainment of EGFR activity as seen through immunoblotting, suggesting the need for further experimental studies

Future Studies: Optimization of liposome incubation protocol; use of scrambled peptide to determine specificity of Sprouty2-derived peptide; binding cell penetrating peptides to the surface of the liposomes to improve efficacy of liposome uptake into the cell

Acknowledgements

R25 Cancer Education Program, Dr. Ceresa's Lab Members
Funding: NIH/NCI R25-CA134283, NIH-GM092874

Is there a Relationship between Patient Worry and Follow-up Care Preferences after Curative Treatment for Lung Cancer?



Ariel M. Washington B.S , Karen Kayser, MSW, PhD , Lisa C. Smith, MSSW, Smita Ranjan, MS, MSN Goetz Kloecker, M.D, MBA, MSPH, FACP
University of Louisville - Kent School of Social Work and School of Medicine



Background

While new methods and techniques are being developed to increase the survivorship rate of lung cancer patients, there is a vast need to aid Kentucky's cancer survivors.

- Kentucky has the highest incidence rate of lung cancer in the country. 97 out of 100,000 residents are diagnosed with lung cancer^{1,2} compared with the national average of 61 per 100,000.
- Lung cancer survivorship is only at 18%.¹
- There lacks a general guideline for oncologists to follow in aiding patients during the transition from curative treatment to surveillance.
- Guidelines of five leading medical organizations (ASCO, ACCP, ESMO, NCCN, ACR) differ about the frequency and the level of imaging and how often follow-up appointments should occur.
- Little consideration is given to the survivor's preferences for follow-up—an important component of patient-centered care.

This study was conducted in an effort to understand the worry that patients experience about recurrence after curative treatment and whether it affects their preferences for treatment.

Research Aims

The aims of this study are to:

1. Describe patients' preferences for medical and supportive care during follow-up treatment;
2. Determine if a relationship exists between patients' preferences for medical follow-up care and their level of fear of recurrence; and
3. Determine if a relationship exists between patients' supportive care preferences and their level of fear of reoccurrence.

Methods

This is a prospective observational study conducted with the James Graham Brown Cancer Center and UofL's Kent School of Social Work. The study is part of a larger longitudinal study investigating the preferences for follow-up care of patients and their primary support persons. After patients had completed their curative treatment and were assessed to be cancer free they were given a survey at their next clinic visit. The questionnaire consisted of several measures focused on their preferences for follow-up regime, quality of life, cancer recurrence worry, physical, emotional and social well being. The Stress and Coping Model was used as a conceptual framework (see Figure 1).

Results

Figure 1: Conceptual Model of Stress and Coping

Adapted from Folkman and Greer, 2000

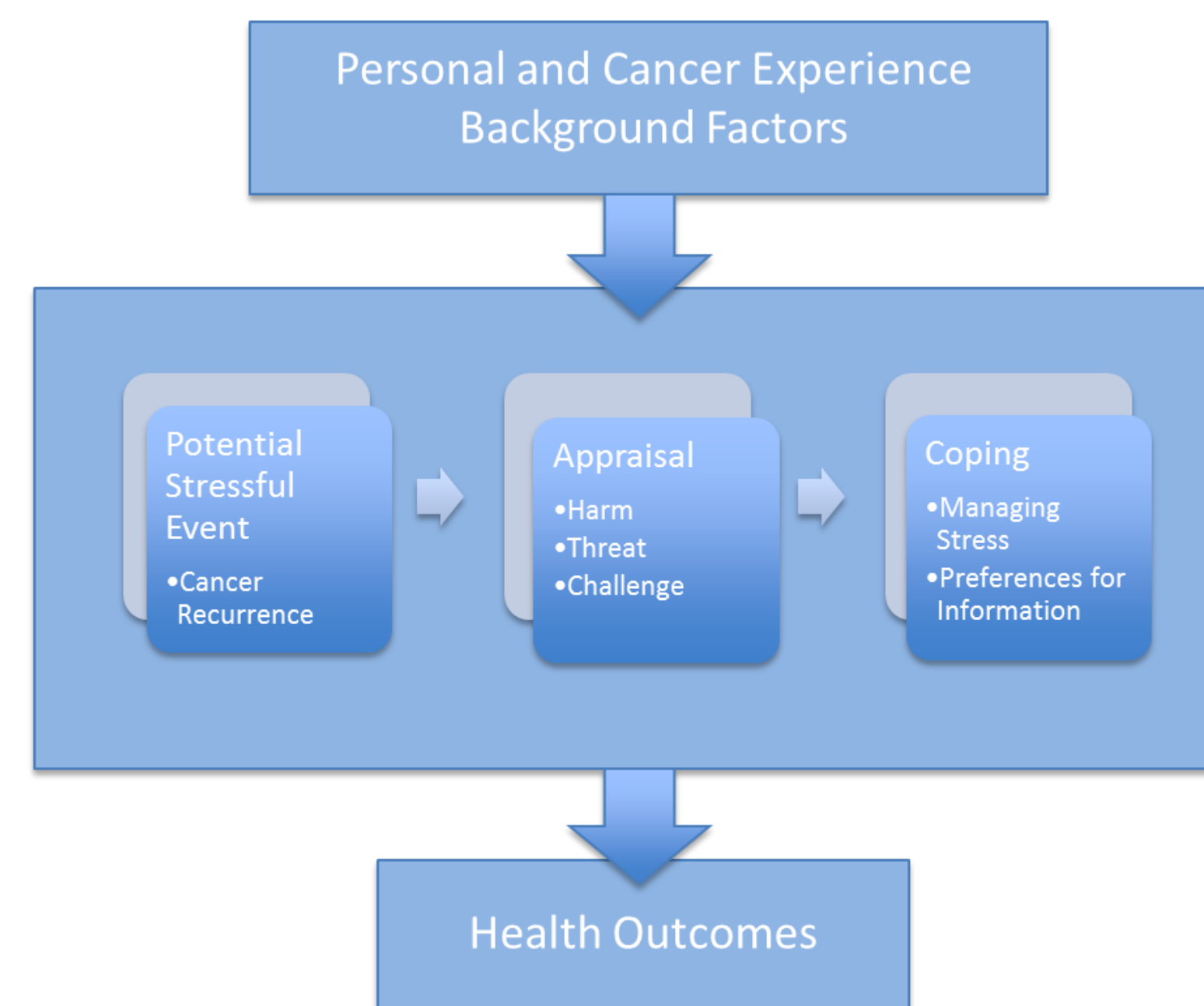


Table 1: Patient Demographics (N=28)

Demographics:	N	%
Gender		
Female	18	64.3
Male	10	35.7
Marital Status		
Married	19	67.8
Not Married	8	28.6
Employment		
Working	7	25
Not Working	19	67.8
Age		
<65	15	53.6
>65	13	46.4
Mean	62.9	
Range	46-82	

Table 2: Correlation of Patient Preferences for Medical-related Follow-up Care with Level of Worry

Preferences for Medical Related Follow-up Care	Fear of Recurrence – Worry
Doctor to check for any signs that the cancer has come back.	0.305
Find out how well I have responded to treatment.	0.295
Find out whether I need to have more treatments.	0.305
Find out more about cancer and its treatment.	0.410*
Discuss planning for the future.	0.450**

Note: *p<.05, **p<.01

Table 3: Frequencies of Patient Preference for medical appointments

Preferences for Timing of Medical Appointments for Follow-up Care	N	%
How soon do you want to have your first follow-up appointment?		
< One Month	2	7.1
One Month	11	39.3
Two Months	4	14.3
>Two Months	6	21.5
How often would you like to have your follow-up appointments?		
Every Three Months	16	57.1
Every Six Months	8	28.6

The majority of the study participants were female, married and not working at time of survey. The average age was 63.5 years.

There were significant correlations between worry and patient's desire for more information about cancer, treatment, and future plans.

Patients did not have a clear consensus on how frequently to conduct follow-up care. However, there was a trend toward a preference for every three months.

Table 4: Correlation of Patient Preferences for Psychosocial Supportive Care with Level of Worry

Preferences for Psychosocial Support Care	Fear of Recurrence - Worry
Discuss how I am coping.	0.438**
Discuss how my family or loved ones are coping.	0.349*
Help with managing feelings of anxiety or sadness.	0.363*
Receive information about what supports are available for my family.	0.428*
Discuss how I can get help at home.	0.048

Note: *p<.05, **p<.01

There were significant correlations between preferences of psychosocial support and worry.

Table 5: Level of Worry about Cancer

Worry Measure Breakdown	Mean
Worry about future diagnostic tests.	2.63
Worry about another type of cancer.	2.59
Worry about cancer coming back.	2.89
Worry about dying.	2.19
Worry about health.	2.92

Patients answered a five-item measure about possible worries with a scale from 1 = not at all worried to 4 = very much worried.

Conclusions

Despite the small sample size, there were some significant relationships between patients' worries about recurrence and their preferences for medical-related follow-up and psychosocial care needs. In particular, those patients who had high levels of worry were more likely to prefer that their follow-up appointments help them and their loved ones to cope better and manage their distress. However, it is noteworthy that very few patients expressed an interest in seeing the social worker for help, although their needs were primarily of a psychosocial nature. Our future research will examine physician preferences for patient follow-up care, screening and referral for psychosocial issues during follow-up, and the development of guidelines for surveillance decision-making.

Acknowledgments

This study was supported by the University of Louisville Cancer Education Program, along with a grant from NIH/NCI

References

1. U.S. Cancer Statistics Working Group. United States Cancer Statistics: 1999–2010 Incidence and Mortality Web-based Report. Atlanta: U.S. Department of Health and Human Services, Centers for Disease Control and Prevention and National Cancer Institute; 2013. Available at: www.cdc.gov/uscs.
2. Kentucky Cancer Registry. Annual Report: Cancer Incidence and Mortality in Kentucky, 2007-2011. Available at www.kcr.uky.edu
3. Folkman, S., & Greer, S. (2000). Promoting psychological well-being in the face of serious illness: When theory, research and practice inform each other. *Psycho-oncology* 9, p. 11-19

Examination of the Cell Cycle Effects of Small Molecule Inhibition of PFKFB4

Lindsey J. Wattley, Jennifer Clark, BA, Erin Ballard, BA, and Sucheta Telang MBBS
 Telang Lab, Molecular Targets
 Brown Cancer Center, University of Louisville

Abstract

Glycolysis despite the presence of oxygen (*i.e.* the Warburg effect) is a metabolic hallmark of cancer cells. 6-Phosphofructo-2-kinase/fructose-2,6-bisphosphatase 4 (PFKFB4), a glycolytic regulating protein, is responsible for converting fructose-6-phosphate (F6P) to fructose-2,6-bisphosphate (F2,6BP) which in turn activates the enzyme 6-phosphofructo-1-kinase (PFK-1).

The requirement of PFKFB4 for cancer cell growth makes this protein a rational drug target. Through *in silico* screening, 5MPN was identified as an inhibitor of the substrate binding site of PFKFB4. We observed that 5MPN decreases cell proliferation by arresting cancer cells in the G0/G1 stage of the cell cycle and sought to further examine the effect.

We used two lung cancer cell lines chosen from an initial screen. We used siRNA to knock down PFKFB4 in each line. Then, we treated each cancer cell line with 5MPN, and the cell cycle effect of the drug was found to mimic siRNA treatment specific to PFKFB4. Finally, we used overexpression of PFKFB4 to rescue the effect of the drug on the cell cycle. Through these analyses we determined that 5MPN decreases cell proliferation in cancer cells by arresting the cells in the G0/G1 phase.

Introduction

Studies have shown that cancer cells take up glucose at a much higher rate than normal cells. According to the Warburg effect, cancer cells preferentially use glycolysis, rather than mitochondrial cellular respiration, even in an abundance of oxygen (1). Therefore, glycolytic regulating proteins have been the targets for new research.

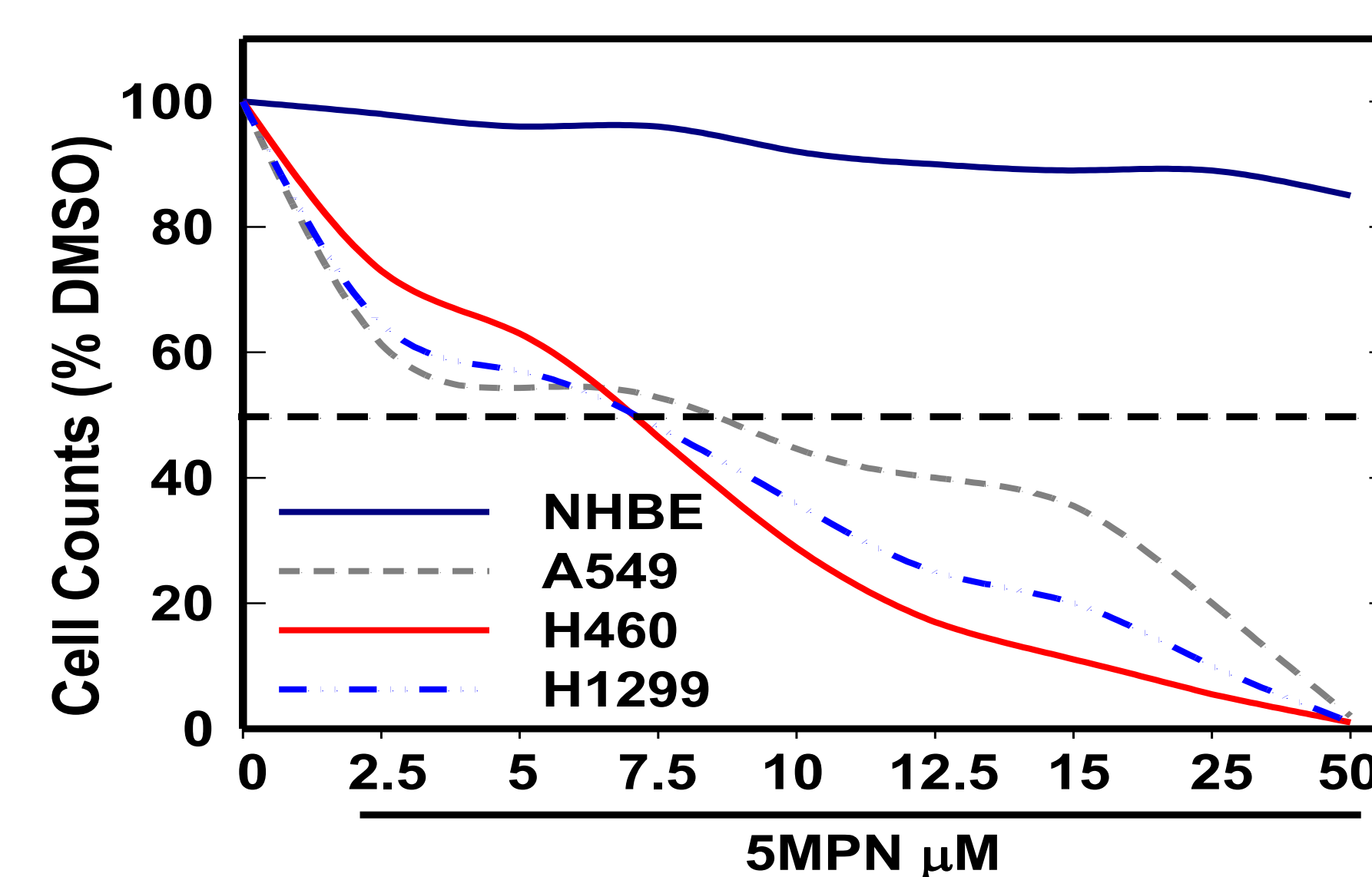
The enzymes PFKFB1-4 are metabolic regulation proteins responsible for interconverting fructose-6-phosphate (F6P) and fructose-2,6-bisphosphate (F2,6BP)(1). F2,6BP in turn activates the enzyme 6-phosphofructo-1-kinase (PFK-1), which increases the rate of change of F6P to fructose-1,6-bisphosphate (F1,6BP), a key step of glycolysis (2).

PFKFB4 has been found to be overexpressed in several cancers particularly under conditions of hypoxia, indicating that this enzyme may play an important role in regulating glycolysis in cancer(3).

In an attempt to inhibit the activity of PFKFB4 and in turn decrease cancer cell growth, an inhibitor (termed 5MPN) was found. Through examination of enzyme kinetic activities, 5MPN has been shown to inhibit the kinase activity of PFKFB4 (unpublished data, Telang *et al*). 5MPN may serve as a future anti-cancer therapeutic.

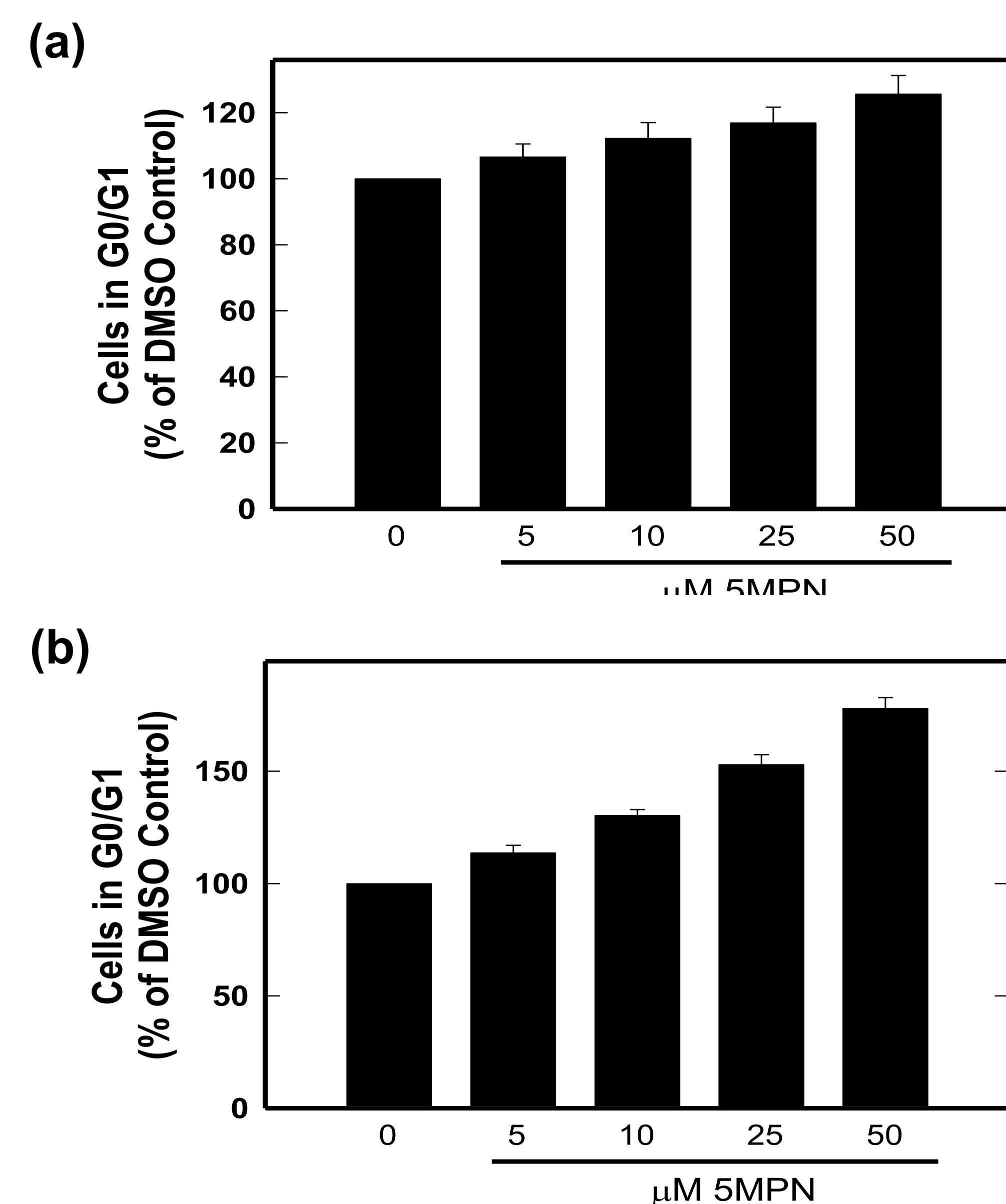
NHBE, A549, H460, H1299 + 5MPN

NHBE, A549, H460, and H1299 cells were treated with 5MPN for 72 hours. The cells were then lifted and counted. The H460 and H1299 had the lowest IC₅₀ of the cell lines examined and therefore were chosen for further investigation.



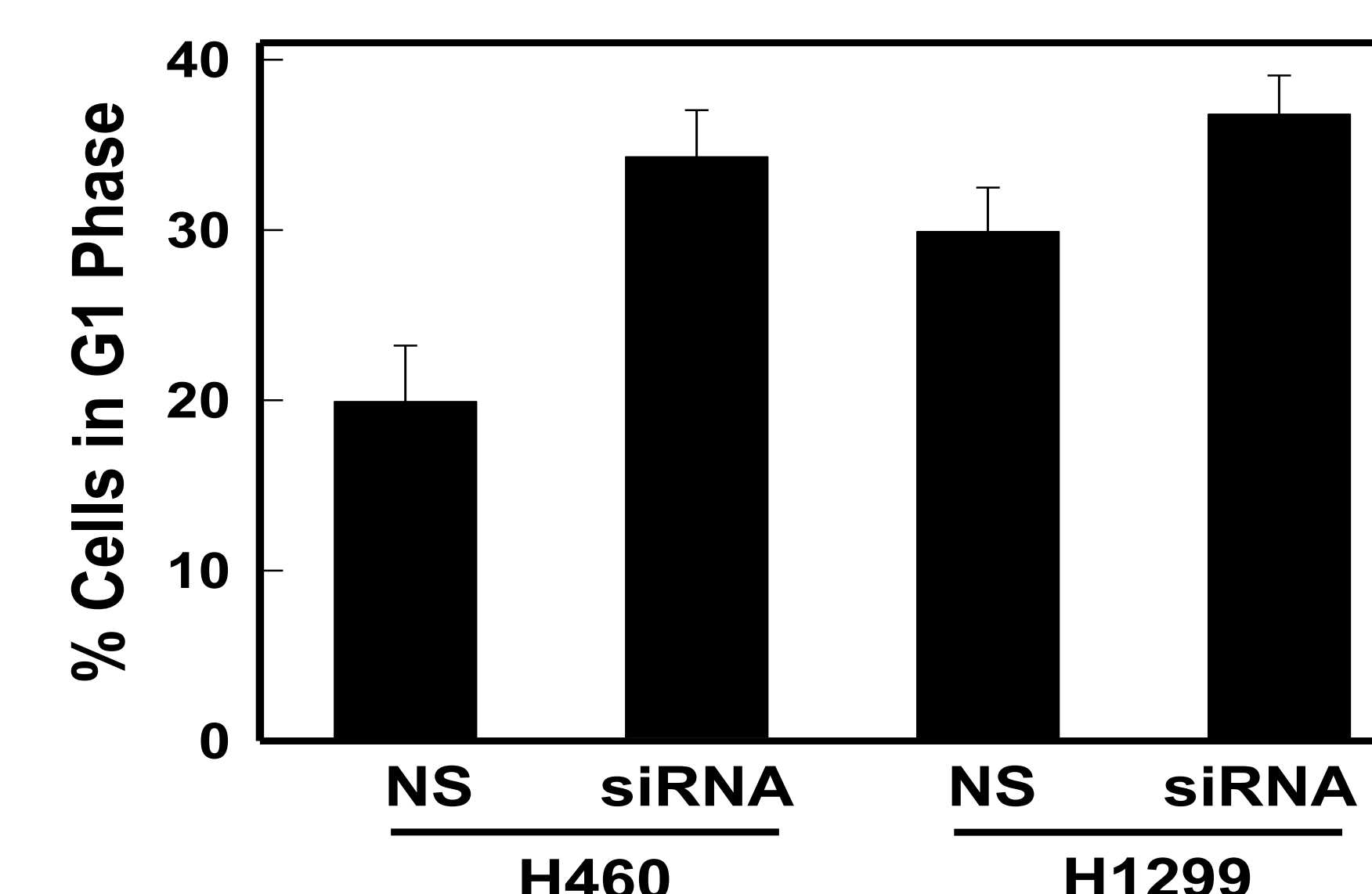
H460 and H1299 + 5MPN

H460 (a) and H1299 (b) cells were treated with 5MPN for 48 hours. The cells were then lifted, fixed in ethanol, plasma and nuclear membranes disrupted by shearing and stained with PI for analysis of cell cycle by flow cytometry.



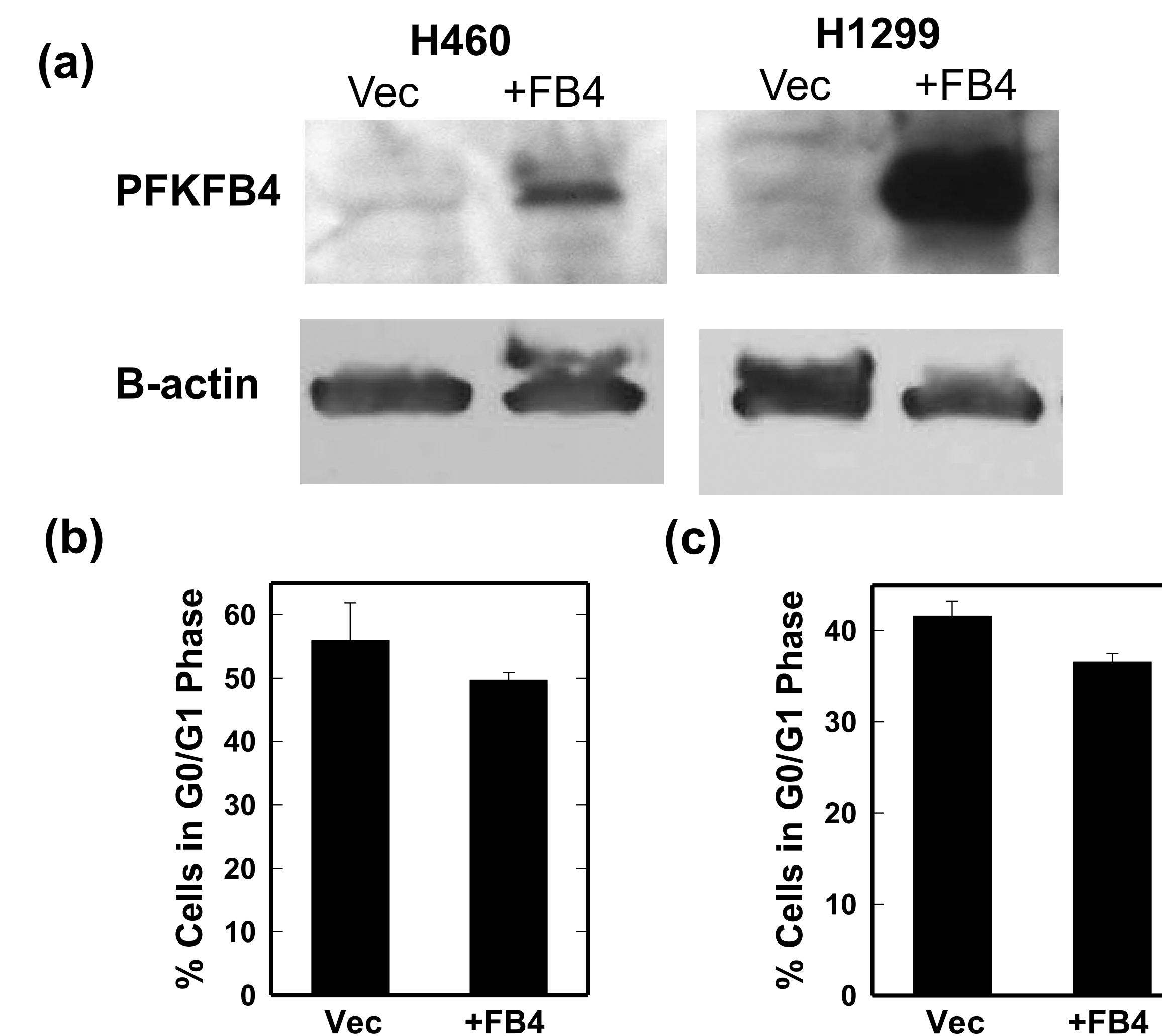
H460, H1299 siRNA

H460 and H1299 cells were transfected with PFKFB4 silencing RNA and nonsense RNA for 6, 12, and 18 hours. The cells were then lifted and cell cycle analyzed by flow cytometry.

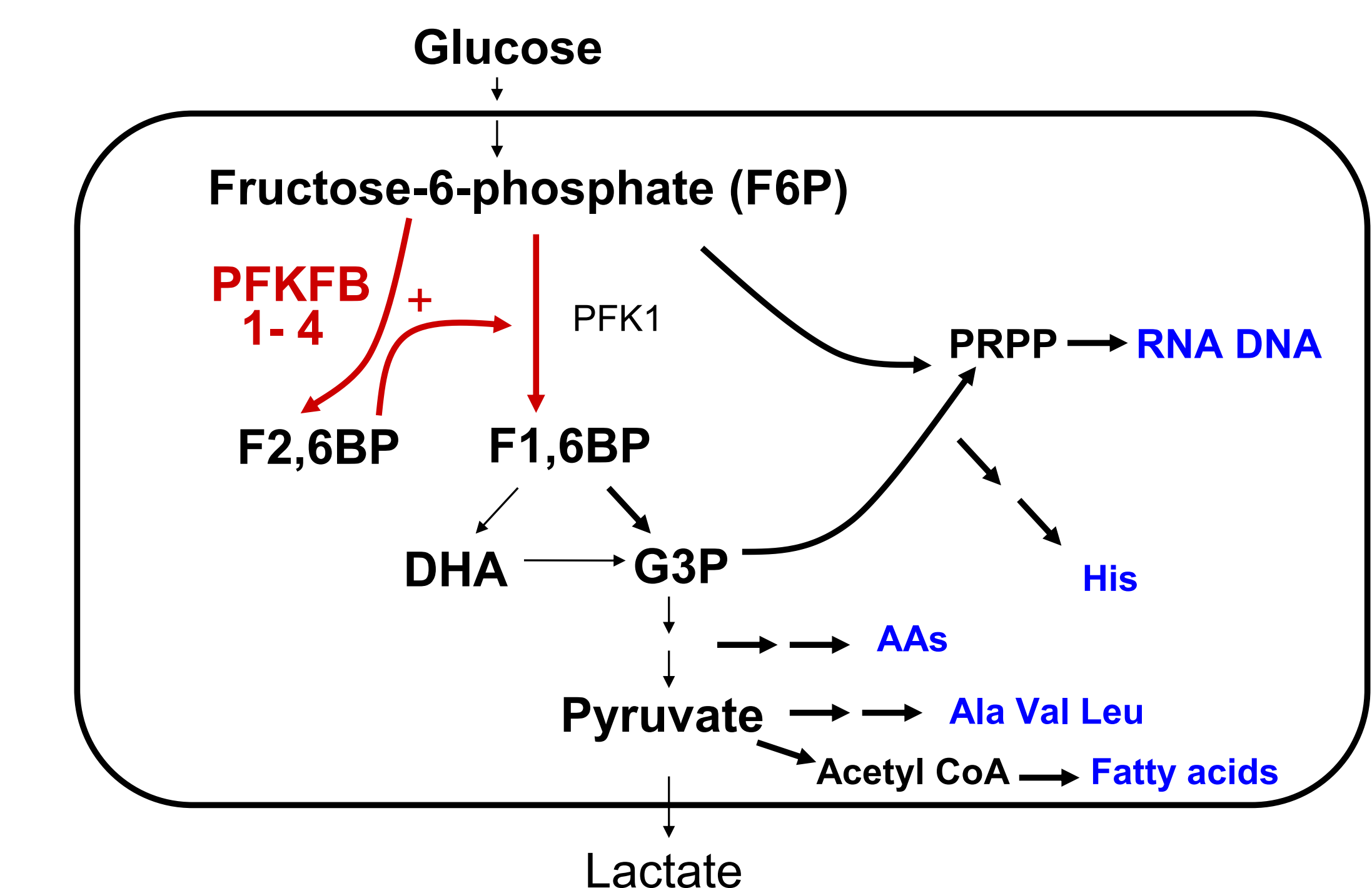


H460, H1299 Overexpression

H460 and H1299 cells were treated with 2.5 μM 5MPN for 48 and 72 hours. After 24 hours of treatment, the cells were transfected with a vector containing PFKFB4 or an empty vector. After 48 and 72 hours, cells were lifted and cell cycle analyzed by flow cytometry. Representative Western blot confirming overexpression shown (a), % of cells in G0/G1 in H460 (b, 72h) and H1299 cells (c, 48h) shown.



PFKFB4 Role in Glycolysis



Conclusion

In conclusion, treatment with 5MPN causes a decrease in cell proliferation by means of a G0/G1 phase arrest. The cell cycle effect of 5MPN mimics the affect of PFKFB4 siRNA, by increasing the amount of G1 and decreasing both S and G2 phases. This cell cycle effect was able to be rescued at low concentrations of 5MPN through an overexpression of PFKFB4.

References

1. Yalcin A., et al., Regulation of glucose metabolism by 6-phosphofructo-2-kinase/fructose-2,6-bisphosphatases in cancer, *Experimental Molecular Pathology* (2009)
2. Clem B., Telang S., Clem A., Yalcin A., Meier J., Simmons A., Rasku M., Arumugam S., Dean W., Eaton J., Lane A., Trent J., Chesney J., Small-molecule inhibitions of 6-phosphofructo-2-kinase activity suppresses glycolytic and tumor growth, *Molecular Cancer Therapeutics* (2008)
3. Minchenko OH et al, Expression and hypoxia responsiveness of 6-phosphofructo-2-kinase/ fructose-2,6-bisphosphatase in mammary gland malignant cell lines. *Acta Biochim Pol.* 2005;52(4):881-8.

Acknowledgements

Support of the Summer Research Intern Lindsey Wattley was partially supported by NCI grant R25 CA134283 to the University of Louisville.